Asymmetric Multiple Description Lattice Vector Quantizers

Suhas N. Diggavi*, N. J. A. Sloane, and Vinay A. Vaishampayan
AT&T Shannon Laboratories,
180 Park Avenue, Bldg 103,
Florham Park NJ 07932, USA.
Tel: (973)-360-8492, FAX: (973)-360-8178.
Email: {suhas,njas,vinay}@research.att.com

Abstract

We consider the design of asymmetric multiple description lattice quantizers that cover the entire spectrum of the distortion profile, ranging from symmetric or balanced to successively refinable. We present a solution to a labeling problem, which is an important part of the construction, along with a general design procedure. The high rate asymptotic performance of the quantizer is also studied. We evaluate the rate-distortion performance of the quantizer and compare it to known information theoretic bounds. The high rate asymptotic analysis is compared to the performance of the quantizer.

Keywords: cubic lattice, lattice quantization, multiple descriptions, high rate quantization, source coding, vector quantization, successive refinement, quantization.

I Introduction

A multiple description source encoder generates a set of binary streams or descriptions of a source sequence, each with its own rate constraint. The transmission medium may

*Contact author, Rm C287, Bldg 103, AT&T Shannon Laboratories, 180, Park Avenue, Florham Park New Jersey, NJ 07932, suhas@research.att.com.

deliver some or all of the descriptions to the decoder. The objective is to minimize the distortion between the source sequence and the decoded sequence when all the descriptions are available, while ensuring that the distortion which results when only a subset of the descriptions are available remains below a pre-specified value that depends on the subset. If there are D descriptions, the *distortion profile* is a vector of length 2^D whose components give the distortion constraints for each subset of the descriptions.

In recent years, multiple description coders have received considerable attention, driven by the interest in packet voice and video communications (see the bibliography). Most of the work (with the exception of [11]) has centered around the successively refinable case and the balanced/symmetric case, which are in a sense two extremes of the distortion profile. Successive refinement coders find application in networks with a priority structure whereas balanced codes are useful in networks that do not have such a structure, the best example at the present time being the Internet.

In this paper we propose a structured scheme that bridges the two cases, in the sense that it permits a fairly general distortion profile to be specified. By allowing the individual descriptions to have different distortions, the quantizer behavior can range from the balanced case (where each description is equally important) to a strict hierarchy (where the loss of some descriptions could make decoding impossible). The new design is described in terms of a lattice vector quantizer, but the general principle of asymmetric multiple description coding can be extended to many other quantizers, such as trellis coded quantizers, unstructured vector quantizers, etc. This could potentially allow us to incorporate channel (or network route) reliability information into the transmission. Also, it might be a useful way to allow for less intrinsic wastage of network traffic as some descriptions could be given to the decoder without necessarily waiting for the more important descriptions to arrive (as in successive refinement).

For previous work on the information theoretic aspects of the multiple description problem see [9, 10, 22, 29, 30]. The problem of designing quantizers for the multiple description problem has been considered in [11, 17, 19, 25, 26, 28]. The work presented in [28] considered only the balanced/symmetric lattice quantizer design. Unlike the work in [11], we do not use a training approach; instead we use the geometry of the underlying lattice to solve a labeling problem. Other approaches to multiple description coding based on overcomplete expansions are presented in [1, 2, 13] and methods based on optimizing transforms and predictors are presented in [16, 21, 27].

The paper is organized as follows. The source coding problem is formulated in Section II, the design method is described in Section III, properties of the lattices and sublattices needed for the construction are developed in Section IV, a high rate analysis is presented in Section V, and numerical results are presented in Section VI.

II Preliminaries

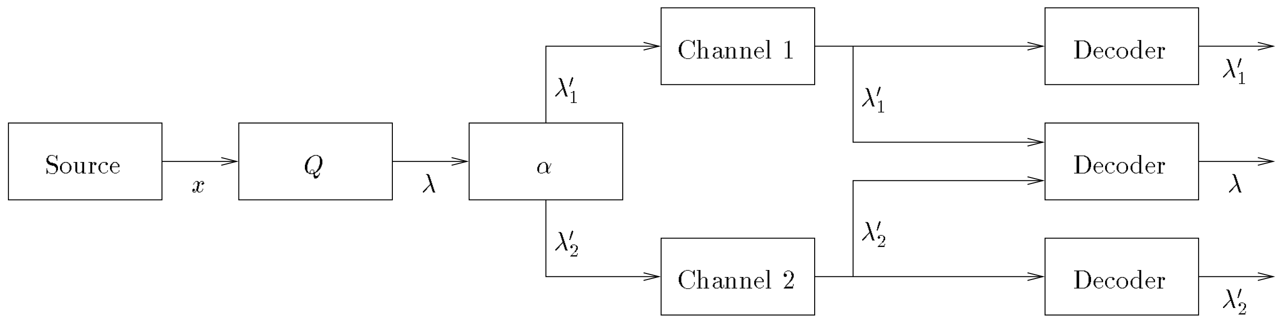

Figure 1: Block diagram of a multiple description vector quantizer.

A block diagram of a two-channel multiple description vector quantizer (MDVQ) using a lattice codebook is shown in Fig. 1. An L-dimensional source vector x is first encoded as the closest vector λ in a lattice $\Lambda \subset \mathbb{R}^L$. We will write $\lambda = Q(x)$. Information about the selected code vector λ is then sent across the two channels, subject to rate constraints imposed by the individual channels. This is done through a labeling function α. At the decoder, if only channel 1 works, the received information is used to select a vector λ_1' from the channel 1 codebook. If only channel 2 works, the information received over channel 2 is used to select a code vector λ_2' from the channel 2 codebook. If both channels work, it is assumed that enough information is available to recover λ.

We will assume that the channel 1 and channel 2 codebooks, denoted by Λ_1 and Λ_2

respectively, are sublattices[1] of Λ. The index $[\Lambda : \Lambda_i]$ is denoted by N_i, $i = 1, 2$. N_i is also called the *re-use index* of sublattice Λ_i. We assume that each Λ_i is *geometrically similar* to Λ, i.e. that Λ_i can be obtained from Λ by applying a *similarity* (a rotation, change of scale and possibly a reflection). To simplify the analysis we will usually assume that the Λ_i are *strictly similar* to Λ, i.e. that reflections are not used.

Property P.1 *Let Λ be an L-dimensional lattice with generator matrix G (the rows of G span Λ). A sublattice $\Lambda_1 \subseteq \Lambda$ is geometrically strictly similar to Λ if and only if the following condition holds: there is an invertible $L \times L$ matrix U_1 with integer entries, a scalar c_1, and an orthogonal $L \times L$ matrix K_1 with determinant 1 such that a generator matrix for Λ_1 can be written as*

$$G_1 = U_1 G = c_1 G K_1 \ . \tag{1}$$

If (1) holds then the index of Λ_1 in Λ is equal to

$$\begin{aligned} N_1 &= [\Lambda : \Lambda_1] = \sqrt{\frac{\det \Lambda_1}{\det \Lambda}} = \frac{\det G_1}{\det G} \\ &= \det U_1 = c_1^L \ . \end{aligned} \tag{2}$$

Furthermore, Λ_1 has Gram matrix

$$A_1 = G_1 G_1^{tr} = U_1 G G^{tr} U_1^{tr} = U_1 A U_1^{tr} = c_1^2 A \ , \tag{3}$$

where $A = GG^{tr}$ is a Gram matrix for Λ.

Even if the similarity is not strict, equations (1), (2) and (3) still hold but with $\det K_1 = -1$. Note that the constant $c_1 > 1$ represents the scaling between the lattice Λ and Λ_1 and thus the index $N_1 = c_1^L$ represents the scaling between the respective volumes of the fundamental regions of the lattices.

We will also usually assume that the sublattices Λ_1 and Λ_2 are *clean* [3], that is, no point of Λ lies on the boundary of the Voronoi cells of Λ_1 or Λ_2. Our algorithm still applies if this condition is not satisfied, but the book-keeping becomes more complicated.

[1] Strictly speaking, the codebooks are finite subsets of the sublattices Λ_1 and Λ_2, but we will ignore that distinction in this paper.

Finally, we require a sublattice of $\Lambda_1 \bigcap \Lambda_2$, Λ_s, (the *product sublattice*) which is geometrically strictly similar to Λ and has index $N_s = N_1 N_2$ in Λ. To reduce the complexity of the design we will also sometimes make use of a sublattice $\Lambda_\cap$ of $\Lambda_1 \bigcap \Lambda_2$ which has index $N_\cap = \text{lcm}(N_1, N_2)$ in Λ (such sublattices do not always exist – see Section IV).

Since the information sent over channel 1 is used to identify a code vector $\lambda_1 \in \Lambda_1$, and the information over channel 2 is used to identify a code vector $\lambda_2 \in \Lambda_2$, we will assume that the labeling function α is a mapping from Λ into $\Lambda_1 \times \Lambda_2$ and that $(\lambda_1, \lambda_2) = \alpha(\lambda)$. The component mappings are $\lambda_1 = \alpha_1(\lambda)$ and $\lambda_2 = \alpha_2(\lambda)$. In order to recover λ when both channels work, it is necessary that α be one-to-one. This is accomplished by requiring that the ordered pair (λ_1, λ_2) is used only once in any labeling scheme.

Given Λ, Λ_1, Λ_2 and α, there are three distortions and two rates associated with the quantizer. For a given source vector x mapped to the triple $(\lambda, \lambda_1, \lambda_2)$, the *two-channel distortion* d_0 is given by $\|x - \lambda\|^2$, the side distortions d_i by $\|x - \lambda_i\|^2$, $i = 1, 2$, where $||\mathbf{x}||^2 \stackrel{\text{def}}{=} (1/L)\sum_{i=1}^{L} x_i^2$ is the dimension-normalized Euclidean norm. The corresponding average distortions are denoted by $\bar{d}_0$, $\bar{d}_1$ and $\bar{d}_2$. (We will also refer to $\bar{d}_0$ as the *central* distortion.) We assume that an entropy coder is used to transmit the labeled vectors at a rate arbitrarily close to the entropy, i.e., $R_i = \mathcal{H}(\alpha_i(Q(\mathbf{X})))/L$, $i = 1, 2$, where $\mathcal{H}$ is the binary entropy function. The problem is to design the labeling function α so as to minimize $\bar{d}_0$ subject to $\bar{d}_1 \leq D_1$ and $\bar{d}_2 \leq D_2$, for given rates (R_1, R_2) and distortions D_1 and D_2.

We will assume that the source is memoryless with probability density function (pdf) p. The L-fold pdf will be denoted by p_L where $p_L((x_1, x_2, \ldots, x_L)) = \prod_{i=1}^{L} p(x_i)$. The differential entropies satisfy the relation $h(p_L) = Lh(p)$.

Given a lattice Λ, a sublattice Λ' and a point $\lambda' \in \Lambda'$, we denote by $V_{\Lambda:\Lambda'}(\lambda')$ the set of all points in Λ that are closer to λ' than to any other point in Λ'. This set is the discrete Voronoi set of λ' in Λ. If Λ' is a clean sublattice of Λ we do not need to worry about ties when calculating $V_{\Lambda:\Lambda'}(\lambda')$. The Voronoi cell $V_\Lambda(\lambda)$ of a point $\lambda \in \Lambda$ is the set of all points in $\mathbb{R}^L$ that are at least as close to λ as to any other point of Λ. Also $\mathcal{E}(\lambda') = \alpha(V_{\Lambda:\Lambda'}(\lambda'))$, $\lambda' \in \Lambda'$, will denote the set of all labels of the points in $V_{\Lambda:\Lambda'}(\lambda')$.

A Distortion Computation

The average two-channel distortion $\bar{d}_0$ is given by

$$\bar{d}_0 = \sum_{\lambda \in \Lambda} \int_{V_\Lambda(\lambda)} \|x - \lambda\|^2 p_L(x) dx. \tag{4}$$

Since the codebook of the quantizer is a lattice, all the Voronoi sets in the above summation are congruent. Furthermore, upon assuming that each Voronoi cell is small and letting ν denote the L-dimensional volume of a Voronoi cell, we obtain the two-channel distortion

$$\bar{d}_0 = \frac{\int_{V_\Lambda(0)} \|x\|^2 dx}{\nu} = G(\Lambda)\nu^{2/L}, \tag{5}$$

where the normalized second moment $G(\Lambda)$ is defined by ([5])

$$G(\Lambda) = \frac{\int_{V_\Lambda(0)} \|x\|^2 dx}{\nu^{1+2/L}}. \tag{6}$$

When only description i is available, for $i = 1, 2$, the distortion is given by

$$\bar{d}_i = \bar{d}_0 + \sum_{\lambda \in \Lambda} \|\lambda - \alpha_i(\lambda)\|^2 P(\lambda), \tag{7}$$

where $P(\lambda)$ is the probability of lattice point λ, and we have assumed that λ is the *centroid* of its Voronoi cell. This is true for the uniform density. For nonuniform densities, there is an error term which goes to zero with the size of the Voronoi cell [14]. The first term in (7) is the two-channel distortion and the second term is the excess distortion which is incurred when only description i is available. Note that, for a given Λ, only the excess distortion term is affected by the labeling α.

At this point we impose a constraint on the labeling function that allows us to reduce the problem to that of labeling a finite number of points. We assume that the labeling function has the *shift invariance* property that $\alpha(\lambda + \lambda_s) = \alpha(\lambda) + \lambda_s$, for all $\lambda_s \in \Lambda_s$. This leads to the following simplification:

$$\bar{d}_i = \bar{d}_0 + (1/N_s) \sum_{\lambda \in V_{\Lambda:\Lambda_s}(0)} \|\lambda - \alpha_i(\lambda)\|^2, \tag{8}$$

where we have assumed that $P(\lambda)$ is approximately constant over a Voronoi cell of the sublattice Λ_s, but may vary from one Voronoi cell to another. The consequence of this structural property is that we focus on the labeling of a set of points in $V_{\Lambda:\Lambda_s}(0)$ and use shifts of this labeling scheme to generate labels for the entire space.

B Rate Computation

Let R_0 bits/sample be the rate required to address the two-channel codebook for a single channel system[2]. We first derive an expression for R_0 and then determine the rates R_1 and R_2. We use the fact that each quantizer bin has identical volume ν and that $p_L(x)$ is approximately piecewise constant over each Voronoi cell of Λ_1 and Λ_2. This assumption is valid in the limit as the Voronoi cells become small and is standard in asymptotic quantization theory.

The rate $R_0 = \mathcal{H}(Q(X))$ is given by

$$\begin{aligned} R_0 &= -(1/L)\sum_{\lambda}\int_{V_\Lambda(\lambda)} p_L(x)dx \log_2 \int_{V_\Lambda(\lambda)} p_L(x)dx \\ &\approx -(1/L)\sum_{\lambda}\int_{V_\Lambda(\lambda)} p_L(x)dx \log_2 p_L(\lambda)\nu \\ &\approx h(p) - (1/L)\log_2(\nu). \end{aligned} \tag{9}$$

It can be shown that the rate for description i is given by

$$R_i = R_0 - (1/L)\log_2(N_i), \quad i = 1, 2\,. \tag{10}$$

A single channel system would have used R_0 bits/sample. Instead a multiple description system uses a total of $R_1 + R_2 = 2R_0 - (1/L)\log_2(N_1 N_2)$ bits/sample, and so the rate overhead is $R_0 - (1/L)\log_2(N_1 N_2)$.

III Construction of the Labeling Function

Suppose Λ is an L-dimensional lattice with a pair of geometrically strictly similar, clean sublattices Λ_1 and Λ_2, and let Λ_s (the product sublattice) be a geometrically strictly similar, clean sublattice of both Λ_1 and Λ_2, with indices $[\Lambda : \Lambda_1] = N_1$, $[\Lambda : \Lambda_2] = N_2$ and $[\Lambda : \Lambda_s] = N_1 N_2$.

In order to construct a labeling function we first identify $\mathcal{E}$, the subset of points of $\Lambda_1 \times \Lambda_2$ that will be used to label the points of Λ. Informally, we call the ordered pair (λ_1, λ_2) an

[2] This quantity is useful for evaluating the two-channel distortion as well as for evaluating the rate overhead associated with the multiple description system.

edge and therefore the labeling function is to associate lattice points with edges. A one-to-one correspondence will be established between $V_{\Lambda:\Lambda_s}(0)$ and a proper subset of $\mathcal{E}$ so as to minimize an appropriate objective function, while ensuring that the labeling can be extended uniquely to the entire lattice. To this end we first start by formulating a cost criterion that will be used in the design.

A Cost criterion

The multiple description problem may be formulated [9] as a problem of minimizing the central distortion subject to constraints on the side distortion. The associated Lagrangian cost criterion is given by

$$\begin{aligned} J &= \bar{d}_0 + \sum_{i=1}^{2} \gamma_i \bar{d}_i \\ &= (\gamma_1 + \gamma_2 + 1)\bar{d}_0 + \sum_{i=1}^{2} \gamma_i \sum_{\lambda \in \Lambda} \|\lambda - \alpha_i(\lambda)\|^2 P(\lambda) \\ &= (\gamma_1 + \gamma_2 + 1)\bar{d}_0 + \sum_{\lambda \in \Lambda} P(\lambda) \sum_{i=1}^{2} \gamma_i \|\lambda - \alpha_i(\lambda)\|^2. \end{aligned} \tag{11}$$

where γ_1, γ_2 are Lagrange multipliers.

The central distortion $\bar{d}_0$ is determined by the lattice Λ. If we assume that $P(\lambda)$ is approximately constant over the Voronoi cell of Λ_s, we can rewrite the cost criterion in terms of the cost over a Voronoi cell of Λ_s. Then the design problem reduces to finding a labeling scheme $\alpha(\lambda)$ which minimizes

$$\frac{1}{N_s} \sum_{\lambda \in V_{\Lambda:\Lambda_s}(0)} \left[\gamma_1 \|\lambda - \alpha_1(\lambda)\|^2 + \gamma_2 \|\lambda - \alpha_2(\lambda)\|^2 \right]. \tag{12}$$

After some algebra, the expression inside the summation can be rewritten as

$$\frac{\gamma_1 \gamma_2}{\gamma_1 + \gamma_2} \|\alpha_2(\lambda) - \alpha_1(\lambda)\|^2 + (\gamma_1 + \gamma_2) \|\lambda - \frac{\gamma_1 \alpha_1(\lambda) + \gamma_2 \alpha_2(\lambda)}{\gamma_1 + \gamma_2}\|^2. \tag{13}$$

The values of γ_1 and γ_2 determine the relative values of the two side-distortions $\bar{d}_1$ and $\bar{d}_2$.

Therefore our design principle is (informally) for a given pair γ_1 and γ_2, to find a labeling function $\alpha(\lambda)$ such that the sublattice points $\alpha_1(\lambda) \in \Lambda_1, \alpha_2(\lambda) \in \Lambda_2$ are not very far apart and the lattice point $\lambda \in \Lambda$ that is being labeled is not very far from the weighted mean (the second term of (13)) of these two sublattice points. This general guiding principle leads to our lattice design. (Note that if we have $\Lambda_1 = \Lambda_2$ then $R_1 = R_2$, although we may still introduce some distortion asymmetry by choosing $\gamma_1 \neq \gamma_2$). We will first describe the basic quantizer design and then illustrate it using the lattice $\mathbb{Z}^2$.

B Lattice Quantizer

The quantizer construction is based on the following steps.

Step 1 We are given an L-dimensional lattice Λ, rates R_1, R_2 and distortions D_1, D_2. These determine the indices N_1, N_2 using (10), and we attempt to find (strictly similar, clean) sublattices Λ_1, Λ_2 with these indices, together with a product sublattice Λ_s. We also choose appropriate values for the weights γ_1 and γ_2. For example, a successively refinable quantizer corresponds to choosing $\gamma_1 = 1$, $\gamma_2 = 0$ and $N_2 = \infty$. For the balanced case we take $\gamma_1 = \gamma_2$. By appropriately choosing $N_1, N_2, \gamma_1, \gamma_2$, one can achieve different levels of asymmetry in rate and distortion.

Step 2 We find the discrete Voronoi set[3] $V_0 \stackrel{def}{=} V_{\Lambda:\Lambda_s}(0)$ for the sublattice Λ_s. This is the fundamental set of points that we will label. The labeling is then extended to the full lattice using the shift invariance property (see Section II). We also find the sets

$$\mathcal{P}_1 = V_{\Lambda_1:\Lambda_s}(0) = V_0 \cap \Lambda_1 \; , \tag{14}$$

$$\mathcal{P}_2 = V_{\Lambda_2:\Lambda_s}(0) = V_0 \cap \Lambda_2 \; , \tag{15}$$

which are the points of Λ_1 and Λ_2 belonging to the Voronoi set V_0.

Step 3 We determine the set

$$\mathcal{L}_1(\lambda_1) = \{\lambda_2 \in \Lambda_2 : \lambda_2 \in V_0 + \lambda_1\} \tag{16}$$

for all $\lambda_1 \in \mathcal{P}_1$. These are the points in the sublattice Λ_2 which are in the Voronoi set V_0 of Λ_s when translated to be centered at $\lambda_1 \in \mathcal{P}_1$. By using these points we ensure

[3] We usually omit the word "discrete" when referring to this set.

that the edge length $\|\alpha_2(\lambda) - \alpha_1(\lambda)\|^2$ will be minimized (see Property P.8). We will show that each member of $\mathcal{L}_1(\lambda_1)$ lies in a different coset with respect to the sublattice shifts in Λ_s (Property P.2). Similarly, we determine the set

$$\mathcal{L}_2(\lambda_2) = \{\lambda_1 \in \Lambda_1 : \lambda_1 \in V_0 + \lambda_2\} \tag{17}$$

for all $\lambda_2 \in \mathcal{P}_2$. The set of edges emanating from V_0 is given by

$$\begin{aligned}\mathcal{E}_{edges} = \{(\lambda_1, \lambda_2) \ : \ \lambda_1 \in \mathcal{P}_1 \ , \ \lambda_2 \in \mathcal{L}_1(\lambda_1)\} \bigcup \\ \{(\lambda_1, \lambda_2) : \lambda_2 \in \mathcal{P}_2 \ , \ \ \lambda_1 \in \mathcal{L}_2(\lambda_2)\} \,.\end{aligned} \tag{18}$$

We find a set of coset representatives $\mathcal{E}_0$ for the equivalence classes of $\mathcal{E}_{edges}$ modulo Λ_s. Property P.6 will establish that we can write $\mathcal{E}_0$ either as

$$\mathcal{E}_0 = \{(\lambda_1, \lambda_2) : \lambda_1 \in \mathcal{P}_1 \text{ and } \lambda_2 \in \mathcal{L}_1(\lambda_1)\} \tag{19}$$

or equally well as

$$\mathcal{E}_0 = \{(\lambda_1, \lambda_2) : \lambda_2 \in \mathcal{P}_2 \text{ and } \lambda_1 \in \mathcal{L}_2(\lambda_2)\} \,. \tag{20}$$

Step 4 Matching the edges to the lattice points in the Voronoi set is now a straightforward and easily solved assignment problem (cf. [18]). The objective is to label each point in V_0 with edges that are distinct modulo Λ_s, in order that the shift invariance property be satisfied. To formulate this assignment problem we compute the cost given by (12) for each lattice point and each equivalence class of edges modulo Λ_s (taking the minimum over the edge class). This allows us to construct the set of edges which will later be used to label the points in $V_{\Lambda:\Lambda_s}$.

If there exists a sublattice $\Lambda_\cap$ (as defined in Section II) which is also a geometrically strictly similar, clean sublattice of Λ_1 and Λ_2 the computational complexity of the design can be further reduced. For then we need only label the points in $V_{\Lambda:\Lambda_\cap}(0)$. We will show that this does not reduce the performance of the quantizer — see Property P.9. In this case we replace the sets $\mathcal{P}_1$ and $\mathcal{P}_2$ by the sets $\mathcal{P}_1' = V_{\Lambda_1:\Lambda_\cap}(0)$ and $\mathcal{P}_2' = V_{\Lambda_2:\Lambda_\cap}(0)$. The rest of the procedure is unchanged.

C Properties of the quantizer

In this section we state some of the properties of the construction proposed in Section B. We have imposed the following restrictions on the labeling scheme:

Constraint 1 The labels satisfy the shift property, *i.e.* $\alpha(\lambda+\lambda_s) = \alpha(\lambda)+\lambda_s, \forall\lambda_s \in \Lambda_s,\ \lambda \in \Lambda$.

Constraint 2 The labels for V_0 lie in different cosets of the product sublattice: i.e. if (λ_1, λ_2) and $(\lambda_1, \lambda_2^{'})$ are valid edges then λ_2 and $\lambda_2^{'}$ are in different cosets with respect to the product sublattice.

Property P.2 *Each member of $\mathcal{L}_1(\lambda_1)$ lies in a different coset with respect to the sublattice shifts in Λ_s, and $|\mathcal{L}_1(\lambda_1)| = N_1$. Similarly each member of $\mathcal{L}_2(\lambda_2)$ lies in a different coset with respect to the sublattice shifts in Λ_s, and $|\mathcal{L}_2(\lambda_2)| = N_2$.*

Proof: Let $\lambda_2, \lambda_2^{'} \in \mathcal{L}_1(\lambda_1)$, and $\lambda_2^{'} = \lambda_2+\lambda_s$ for some $\lambda_s \in \Lambda_s$. Then $\lambda_2^{'}-\lambda_1 = \lambda_2-\lambda_1+\lambda_s$. Hence $\lambda_2-\lambda_1$ and $\lambda_2^{'}-\lambda_1$ cannot both lie in V_0. But since $\lambda_2, \lambda_2^{'} \in \mathcal{L}_1(\lambda_1)$, $\lambda_2-\lambda_1$ and $\lambda_2^{'}-\lambda_1$ are in V_0, a contradiction. Thus each $\lambda_2 \in \mathcal{L}_1(\lambda_1)$ is in a different coset with respect to the sublattice shifts in Λ_s. Now $\{V_0 + \lambda_1^{'}\}_{\lambda_1^{'}=\lambda_1+\lambda_s, \lambda_s\in\Lambda_s}$ is a partitioning of the points of Λ, and each of these disjoint sets contains points from different cosets of Λ_2 (with respect to shifts in Λ_s). Since there are only N_1 different cosets of Λ_2, $|\mathcal{L}_1(\lambda_1)| \leq N_1$. In fact equality must hold, because the space is tiled by such sets and if there were a $\lambda_1^{'}$ for which $|\mathcal{L}_1(\lambda_1^{'})| < N_1$ then would be a λ_1 for which $|\mathcal{L}_1(\lambda_1)| > N_1$, which impossible. An identical proof holds for $\mathcal{L}_2(\lambda_2)$. ■

Property P.3 *$\mathcal{L}_1(\lambda_1)$ consists of the N_1 points $\lambda_2 \in \Lambda_2$ closest to λ_1 subject to the constraint that each λ_2 is in a different coset.*

Proof: We know that $\lambda_2 \in \mathcal{L}_1(\lambda_1) \Leftrightarrow \lambda_2 \in V_0 + \lambda_1 \Leftrightarrow \lambda_2 - \lambda_1 \in V_0$. Then $\lambda_2 - \lambda_1 \in V_0 \Leftrightarrow ||\lambda_2 - \lambda_1||^2 \leq ||\lambda_2 - \lambda_1 + \lambda_s||^2$, for all $\lambda_s \in \Lambda_s$. Thus for any $\lambda_2^{'} = \lambda_2 + \lambda_s, \lambda_s \neq 0$ we have $||\lambda_2 - \lambda_1||^2 \leq ||\lambda_2^{'} - \lambda_1||^2$, and the claim follows. ■

Property P.4 $\lambda_2 \in \mathcal{L}_1(\lambda_1) \Leftrightarrow \lambda_1 \in \mathcal{L}_2(\lambda_2)$.

Proof: For clean lattices, if $x \in V_0$ then $-x \in V_0$ [5]. Then $\lambda_2 \in \mathcal{L}_1(\lambda_1) \Leftrightarrow \lambda_2 \in V_0 + \lambda_1 \Leftrightarrow \lambda_2 - \lambda_1 \in V_0 \Leftrightarrow \lambda_1 - \lambda_2 \in V_0 \Leftrightarrow \lambda_1 \in V_0 + \lambda_2 \Leftrightarrow \lambda_1 \in \mathcal{L}_2(\lambda_2)$. ■

Property P.5 *As lattice points in Λ are labeled, the number of times each point from Λ_1 is used is N_1 and the number of times each point from Λ_2 is used is N_2.*

Proof: Let $N(\lambda_1)$ denote the number of lattice points labeled by $\lambda_1 \in \Lambda_1$. Certainly $N(\lambda_1) \geq N_1$ since λ_1 is used N_1 times when we form the edges $\{(\lambda_1, \lambda_2) : \lambda_2 \in \mathcal{L}_1(\lambda_1)\}$. If λ_1 is used in more than N_1 labels then there is a valid edge (λ_1, λ_2) with $\lambda_2 \notin \mathcal{L}_1(\lambda_1)$. But this is impossible by Property P.4. Therefore $N(\lambda_1) = N_1$ for all $\lambda_1 \in \Lambda_1$ and similarly $N(\lambda_2) = N_2$ for all $\lambda_2 \in \Lambda_2$. ■

Property P.6 *The number of cosets in the edge set $\mathcal{E}_0$ modulo Λ_s is equal to the number of lattice points in V_0.*

Proof: Consider the edge set $\mathcal{E}_0 = \{(\lambda_1, \lambda_2) : \lambda_1 \in \mathcal{P}_1, \lambda_2 \in \mathcal{L}_1(\lambda_1)\}$. From Property P.2 each $\lambda_2 \in \mathcal{L}_1(\lambda_1)$ lies in a different coset modulo Λ_s and hence each edge $(\lambda_1, \lambda_2) \in \mathcal{E}_0^{(1)}$ lies in a different coset. As $|\mathcal{E}_0^{(1)}| = N_1 N_2$, there are at least that many cosets in the edge set. ■

Property P.7 *The labeling scheme produces a unique label for each lattice point.*

Proof: This is immediate from the fact that the labels for the cosets of Λ/Λ_s are taken from distinct cosets of $\mathcal{E}_0/\Lambda_s$. ■

Property P.8 *The labeling scheme minimizes the cost criterion given in* (11) *subject to the coset restriction.*

Proof: This is an immediate consequence of Property P.3. ■

Property P.9 *Suppose N_1 and N_2 are not relatively prime, and there exists a sublattice $\Lambda_\cap$ with index lcm$\{N_1, N_2\}$ in Λ which is a geometrically strictly similar, clean sublattice of Λ_1 and Λ_2, and contains Λ_s. Then we may construct the labeling to be invariant under shifts by $\Lambda_\cap$, and obtain the same edge set as if we used the product lattice Λ_s. With this procedure it is necessary to label only lcm$\{N_1, N_2\}$ lattice points rather than $N_1 N_2$ points.*

Proof: If such a $\Lambda_\cap$ exists then we just need to show that the edge set constructed by using the algorithm with Λ_s can be produced by sublattice shifts of the edge set constructed using $\Lambda_\cap$. As we saw in the proof of Property P.6, the coset representatives for the edge set are constructed by using $\mathcal{E}_0 = \{(\lambda_1, \lambda_2) : \lambda_1 \in \mathcal{P}_1, \lambda_2 \in \mathcal{L}_1(\lambda_1)\}$, where $\mathcal{P}_1 = \bigcup_{\lambda_\cap \in \Lambda_\cap} \bigcup_{\lambda_1 \in \mathcal{P}_1'} (\lambda_1 + \lambda_\cap)$. Therefore $\mathcal{E}_0 = \bigcup_{\lambda_\cap \in \Lambda_\cap} \mathcal{E}_0'$, where $\mathcal{E}_0' = \{(\lambda_1, \lambda_2) : \lambda_1 \in \mathcal{P}_1', \lambda_2 \in \mathcal{L}_1(\lambda_1)\}$, where $\mathcal{P}_1' = V_{\Lambda_1 : \Lambda_\cap}(0)$. It follows that there are exactly lcm $\{N_1, N_2\}$ coset leader edges in $\mathcal{E}_0$ with respect to the sublattice $\Lambda_\cap$ and they are given in $\mathcal{E}_0'$. Therefore, by matching the cosets of the edges modulo $\Lambda_\cap$ with the lattice points in the Voronoi set for $\Lambda_\cap$, using the assignment algorithm (as before), and then shifting by $\Lambda_\cap$ we produce exactly the same labeling as we obtained using Λ_s. ■

The property P.9 illustrates that we can reduce computational complexity in the design of the quantizer by using the shift-invariance property of the design over a smaller set of points without any sacrifice in performance. The following property P.10 can be used to obtain a finer scale of global asymmetry by mixing configurations with different levels of asymmetry. For example by equally mixing configurations with complementary distortion ratios, we can create globally symmetric side distortions. We call the weighted average of the lattice points, $\frac{\gamma_1 \lambda_1 + \gamma_2 \lambda_2}{\gamma_1 + \gamma_2}$, *representation points* as they are chosen to be close to the lattice point that the edge represents. Note that distinct edges may share representation points.

Property P.10 *If there exist several labeling schemes achieving the same cost we can mix these configurations to achieve different levels of asymmetry. A sufficient condition for this to occur is for the number of unique representation points to be smaller than the number of lattice points in the product lattice Λ_s.*

Proof: The number of representation points is equal to the number of lattice points in the Voronoi set V_0 (see Property P.6). Therefore, if there are some representation points which overlap (*i.e.* the number of unique representation points is less than the number of points in V_0), then there is more than one labeling scheme that produces the same Lagrangian $\gamma_1 \bar{d}_1 + \gamma_2 \bar{d}_2$, with each labeling producing different $\bar{d}_1, \bar{d}_2$. Suppose one extremal configuration produces the lowest $\bar{d}_1^{min}$ and (therefore) the largest $\bar{d}_2^{max}$, and another extremal configuration produces the highest $\bar{d}_1^{max}$ and the lowest $\bar{d}_2^{min}$. Then by using the first configuration in proportion α and the second in proportion $\bar{\alpha} = 1 - \alpha$ one can produce side distortions $\bar{d}_1 = \alpha \bar{d}_1^{min} + \bar{\alpha} \bar{d}_1^{max}$ and $\bar{d}_2 = \alpha \bar{d}_2^{max} + \bar{\alpha} \bar{d}_2^{min}$. Thus by keeping the Lagrangian cost the same, one can obtain different levels of asymmetry in the distortions $\bar{d}_1, \bar{d}_2$. ∎

The case of the scalar quantizer ($L = 1$) is of particular interest as these are widely used in practice. For a scalar quantizer, $\Lambda = \mathbb{Z}$ with $\Lambda_1 = N_1\mathbb{Z}$, $\Lambda_2 = N_2\mathbb{Z}$, $\Lambda_\cap = \text{lcm}(N_1, N_2)\mathbb{Z}$ and $\Lambda_s = N_1 N_2 \mathbb{Z}$. The points of $\lambda_2 \in \Lambda_2$ closest to a point $\lambda_1 \in \Lambda_1$ are in different cosets with respect to the lattice Λ_s. Therefore the edge selection procedure outlined in Section IIIB is optimal, in that the quantizer design produces the smallest cost as given by (12).

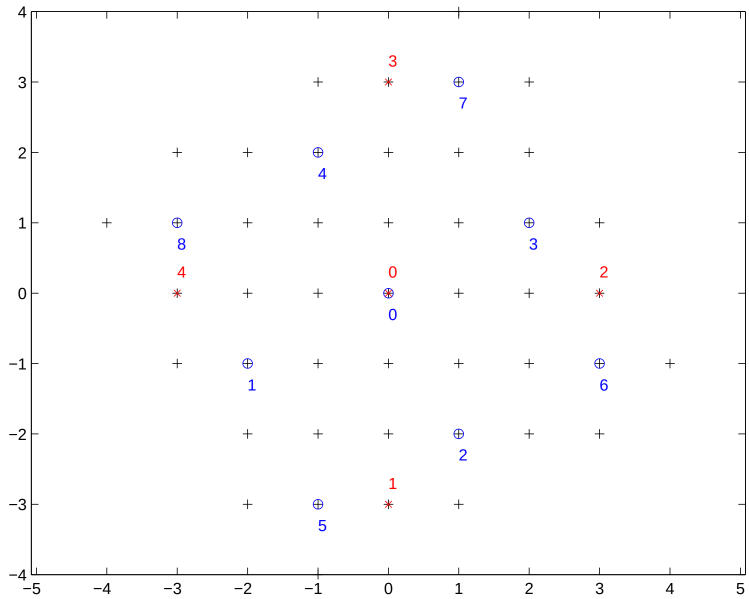

Figure 2: Elements of Λ_1 and Λ_2 in Voronoi set V_0 of Λ_s.

D Example

In this section we illustrate the design procedure with an example in two dimensions using the lattice $\mathbb{Z}^2$. We choose $|\Lambda_1| = 5$ and $|\Lambda_2| = 9$. Portions of the two sublattices are shown in Figure 2 where the points of Λ_1 are marked with circles, the points of Λ_2 with asterisks, and the points of Λ_s with both circles and asterisks. [4] There are 45 points in the Voronoi set V_0 for Λ_s. The set $\mathcal{P}_1$ contains 9 points of Λ_1 and the set $\mathcal{P}_2$ contains 5 points of Λ_2.

[4] In the enhanced (pdf) version of this document the circles are blue and the crosses are red.

The edges $\mathcal{E}_{edges}$ (see Eq. (18)) emanating from the points of V_0 are shown in Figure 3. These are found using the sets $\mathcal{L}_1(\lambda_1)$ and $\mathcal{L}_2(\lambda_2)$ for $\lambda_1 \in \Lambda_1$, $\lambda_2 \in \Lambda_2$. For example, if we take the point $\lambda_1 = (2,1) \in \mathcal{P}_1$, we see that there are 5 points in the set $\mathcal{L}_1(\lambda_1)$, namely $\{(0,0),(0,3),(3,3),(6,0),(3,0)\}$. Note that there are several edges emanating from V_0 which are a sublattice Λ_s shift apart. For example the edge $\{(-2,-1),(-6,0)\}$ is a sublattice Λ_s shift away from the edge $\{(4,2),(0,3)\}$. To satisfy the shift invariance constraint, we must use only one of these edges to label a point in V_0. This constraint is built into the optimization procedure. The result of the optimization procedure is illustrated in Figure 4. Here we have shown only the points in Λ_0. The points in $\Lambda_1 \cap \Lambda_0$ are marked by circles and those in $\Lambda_2 \cap \Lambda_0$ by asterisks. Each point carries a pair of labels (λ_1, λ_2) with $\Lambda_1 \in \Lambda_1$, $\lambda_2 \in \Lambda_2$. The complete listing of the labeling is given in Table 1. In this example we have set $\gamma_1 = 9$ and $\gamma_2 = 5$, which determines the respective distortions $\bar{d}_i$ obtained by the design. A comparison of these distortions with that predicted by information theory is given in Section VI.

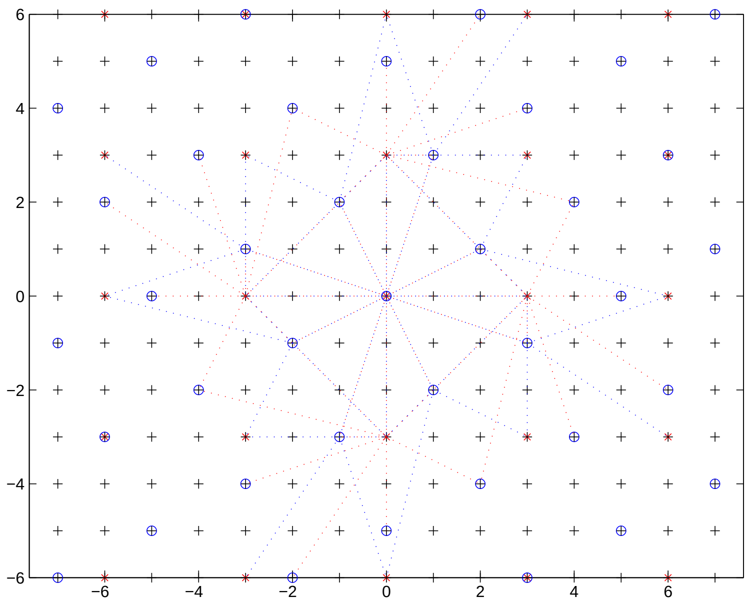

Figure 3: Edges emanating from the Voronoi cell of the sublattice.

λ	λ_1	λ_2	λ	λ_1	λ_2	λ	λ_1	λ_2
(0,0)	(0,0)	(0,0)	(-1,0)	(0,0)	(-3,0)	(0,-1)	(0,0)	(0,-3)
(1,0)	(0,0)	(3,0)	(0,1)	(0,0)	(0,3)	(-1,-1)	(-2,-1)	(0,0)
(-1,1)	(-1,2)	(0,0)	(1,-1)	(1,-2)	(0,0)	(1,1)	(2,1)	(0,0)
(-2,0)	(-3,1)	(0,0)	(0,-2)	(-1,-3)	(0,0)	(2,0)	(3,-1)	(0,0)
(0,2)	(1,3)	(0,0)	(-2,1)	(-1,2)	(-3,0)	(1,-2)	(1,-2)	(0,-3)
(-2,-1)	(-2,-1)	(-3,0)	(2,-1)	(1,-2)	(3,0)	(2,1)	(2,1)	(3,0)
(-1,2)	(-1,2)	(0,3)	(-1,-2)	(-2,-1)	(0,-3)	(1,2)	(2,1)	(0,3)
(2,-2)	(1,-2)	(3,-3)	(-2,-2)	(-2,-1)	(-3,-3)	(-2,2)	(-1,2)	(-3,3)
(2,2)	(2,1)	(3,3)	(0,-3)	(-1,-3)	(0,-3)	(3,0)	(3,-1)	(3,0)
(-3,0)	(-3,1)	(-3,0)	(0,3)	(1,3)	(0,3)	(3,-1)	(3,-1)	(3,-3)
(-3,-1)	(-2,-1)	(-6,0)	(1,-3)	(1,-2)	(0,-6)	(-1,-3)	(-1,-3)	(-3,-3)
(-3,1)	(-3,1)	(-3,3)	(-1,3)	(-1,2)	(0,6)	(3,1)	(2,1)	(6,0)
(1,3)	(1,3)	(3,3)	(-3,2)	(-4,3)	(-3,0)	(3,-2)	(4,-3)	(3,0)
(-2,-3)	(-3,-4)	(0,-3)	(2,3)	(3,4)	(0,3)	(-4,1)	(-5,0)	(-3,3)
(4,-1)	(5,0)	(3,-3)	(-1,-4)	(0,-5)	(-3,-3)	(1,4)	(0,5)	(3,3)

Table 1: Lattice points and labels for a Voronoi set of the product sublattice as labeled in Figure 4.

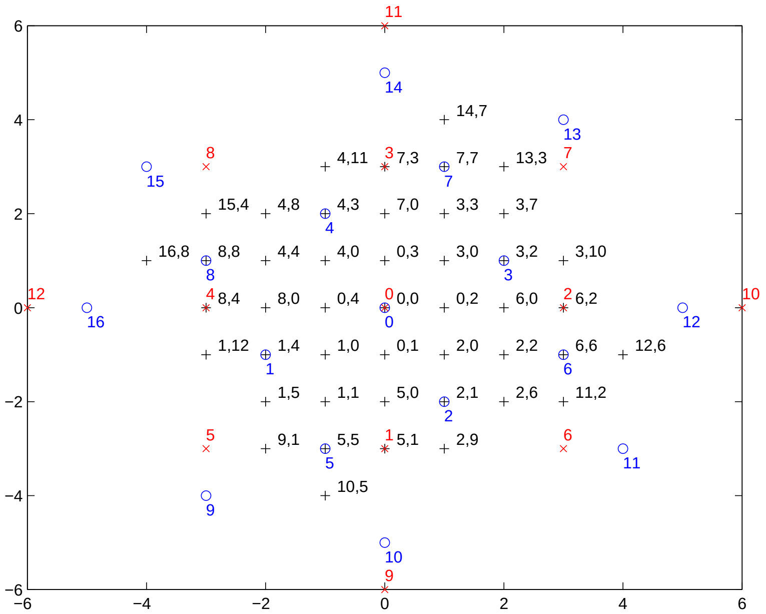

Figure 4: Labels generated by the algorithm.

IV Good lattices

The lattices that we will investigate and apply in this paper are $\mathbb{Z}^n$ for $n = 1, 2$ or a multiple of 4, together with the root lattices D_4 and E_8 [5]. The analysis could be extended to treat other lattices such as $\mathbb{Z}^3$, $\mathbb{Z}^6$, the 12-dimensional Coxeter-Todd lattice, the 16-dimensional Barnes-Wall lattice or the 24-dimensional Leech lattice ([5], [20]), but we shall not discuss these here.

A The construction of similar sublattices

We begin with the observation that multiplication of points in the square lattice $\mathbb{Z}^2$ (regarded as points in the complex plane) by $1 + i$ produces a similar sublattice of index 2. All our sublattices will be constructed by generalizing this remark.

We will make use of five types of integers: $\mathbb{Z}$, the ordinary *rational integers*; $\mathcal{G}$, the ring of *Gaussian integers* $\{a + bi : a, b \in \mathbb{Z}\}$, where $i = \sqrt{-1}$; $\mathcal{J}$, the ring of *Eisenstein integers* $\{a + b\omega : a, b \in \mathbb{Z}\}$, where $\omega = e^{2\pi i/3}$; $\mathbb{H}_0$, the ring of *Lipschitz integral quaternions* $\{a + bi + cj + dk : a, b, c, b \in \mathbb{Z}\}$, where i, j, k are the familiar unit quaternions; and $\mathbb{H}_1$, the ring of *Hurwitz integral quaternions* $\{a + bi + cj + dk : a, b, c, d$ all in $\mathbb{Z}$ or all in $\mathbb{Z} + \frac{1}{2}\}$. Other rings of integers could also be used, but these suffice for the lattices considered in this paper.

If $\Lambda = \mathbb{Z}$, multiplication of lattice points by $\xi \in \mathbb{Z}$ gives $\xi\mathbb{Z}$, a similar sublattice of index $N = |\xi|$.

If $\Lambda = \mathbb{Z}^2 = \mathcal{G}$, multiplication by the Gaussian integer $\xi = a + bi \in \mathcal{G}$ gives a similar sublattice $\Lambda' = \xi\Lambda$ of index $N = a^2 + b^2$. A number N is of the form $a^2 + b^2$ if and only if it is of the form

$$2^{e_1} \prod_{p_i \equiv 1 (4)} p_i^{f_i} \prod_{q_j \equiv 3 (4)} q_j^{2g_j} , \tag{21}$$

where the first product is over primes p_i congruent to 1 (mod 4), the second product is over primes q_j congruent to 3 (mod 4) and e_1, f_i and g_j are nonnegative integers. These indices are the numbers

$$1, 2, 4, 5, 8, 9, 10, 13, 16, 17, 18, 20, \ldots \tag{22}$$

(Sequence A1481 of [24]).

If $\Lambda = A_2 = \mathcal{J}$, the planar hexagonal lattice, multiplication by the Eisenstein integer $\xi = a + b\omega \in \mathcal{J}$ gives a similar sublattice $\Lambda' = \xi\Lambda$ of index $N = a^2 + ab + b^2$. A number N is of the form $a^2 + ab + b^2$ if and only if primes congruent to 2 (mod 3) appear to even powers. These indices are the numbers

$$1, 3, 4, 7, 9, 12, 13, 16, 19, 21, 25, 27, \ldots \tag{23}$$

(Sequence A3136 of [24]).

It is shown in [3] that the above conditions are also necessary: if $\mathbb{Z}, \mathbb{Z}^2$ or A_2 has a similar sublattice of index N then N must have the form described in the preceding paragraphs.

For the lattices $\Lambda = \mathbb{Z}^4$, $\mathbb{Z}^8$, $\mathbb{Z}^{12}, \ldots, D_4$ and E_8 a necessary condition for the existence of a geometrically similar sublattice of index N is that N should be of the form $m^{L/2}$ for some integer m, where L is the dimension. This condition is also sufficient, since such sublattices can be obtained by writing $m = a^2 + b^2 + c^2 + d^2$, regarding Λ as a sublattice of $\mathbb{H}_0^{L/4}$, and multiplying Λ on the left or on the right by the quaternion $\xi = a + bi + cj + dk$. Left and right multiplications in general give different sublattices. In the case of D_4 and E_8 we may also multiply by Hurwitz integral quaternions to obtain further similar sublattices.

Odd-dimensional lattices of dimension greater than 1 are less interesting. For a lattice Λ of odd dimension L has a geometrically similar sublattice of index N if and only if N is an L-th power, say m^L, and sublattices of this index can be obtained by scalar multiplication of Λ by m (see [3]).

The *norm* of a quaternion $\xi = a + bi + cj + dk$ is $\xi\bar{\xi} = a^2 + b^2 + c^2 + d^2$ where the bar denotes quaternionic conjugation. If ξ belongs to one of the above rings, the index of the sublattice $\xi\Lambda$ (or $\Lambda\xi$) in Λ, $[\Lambda : \xi\Lambda]$, is equal to $(\xi\bar{\xi})^{L/2}$, where L is the dimension and the bar is complex or quaternionic conjugation as appropriate.

B Clean sublattices

In dimension one, the sublattice $\xi\mathbb{Z}$ is clean if and only if ξ is odd.

Reference [3] gives necessary and sufficient conditions for a similar sublattice of any two-dimensional lattice to be clean. In particular, the sublattice $\xi\mathbb{Z}^2$ ($\xi = a + ib$) is clean if and only if $N = a^2 + b^2$ is odd. These indices are obtained by setting $e_1 = 0$ in (21):

$$1, 5, 9, 13, 17, 25, 29, 37, 41, 45, \ldots$$

(Sequence A57653).

The sublattice ξA_2 ($\xi = a + b\omega$) is clean if and only if a and b are relatively prime. It follows that A_2 has a clean similar sublattice of index N if and only if N is a product of primes congruent to 1 (mod 6). These are the numbers

$$1, 7, 13, 19, 31, 37, 43, 49, 61, 67, \ldots \tag{24}$$

(Sequence A57654).

The existence of clean sublattices in dimensions greater than 2 was not considered in [3]. We can give a fairly complete answer for the lattices $\mathbb{Z}^L$, $L \geq 1$.

Theorem IV.1 *Suppose $L \geq 1$ and $\mathbb{Z}^L$ has a geometrically similar sublattice Λ' of index N. Then Λ' is clean if and only if N is odd.*

Proof. (If) Let $\Lambda' = \phi(\mathbb{Z}^L)$, where ϕ is a similarity, and let $\Lambda'' = \phi^{-1}(\mathbb{Z}^L)$. If ϕ multiplies lengths by c_1 (as in (1)) then $N = c_1^L$. Suppose $N = c_1^L$ is odd and let Λ' have generator matrix K, with $KK^{tr} = c_1^2 I_L = mI_L$, where $m = c_1^2$. (In the notation of (1), $U_1 = c_1 K_1 = K$.) Note that as KK^{tr} has integer entries, $m = c_1^2$ is an integer and as $N^2 = m^L$ is odd, so is m. Since Λ' is a sublattice of $\mathbb{Z}^L$, the entries of K are integers. Then Λ'' has generator matrix $K^{-1} = \frac{1}{m}K^{tr}$.

We must show that there are no points of $\mathbb{Z}^L$ on the boundary of the Voronoi cell of Λ', or equivalently that there are no points of Λ'' on the boundary of the Voronoi cell of $\mathbb{Z}^L$.

It is enough to consider just one face of the Voronoi cell of $\mathbb{Z}^L$, say that consisting of the points $P = \left(\frac{1}{2}, \frac{x_2}{2}, \frac{x_3}{2}, \ldots, \frac{x_L}{2}\right)$, where $|x_i| \leq 1$ for $2 \leq i \leq L$. If $P \in \Lambda''$ then there is a vector $u = (u_1, \ldots, u_L) \in \mathbb{Z}^L$ such that

$$P = \frac{1}{m} u K^{tr} \ . \tag{25}$$

Equating the first components we get that

$$\frac{1}{2} = \frac{1}{m} \text{ times a vector with integer entries .}$$

Since m is odd this is impossible.

(Only if) Suppose N is even, then as $N^2 = m^L$, m is also an even integer. We claim that all the vertices of the Voronoi cell for $\mathbb{Z}^L$ (i.e. all the deep holes in $\mathbb{Z}^L$ in the notation of [5]) belong to Λ''. In fact, (25) implies that $u = PK$. Let P be a vector of the form $(\pm\frac{1}{2}, \pm\frac{1}{2}, \ldots, \pm\frac{1}{2})$, and let $K = (k_{ij})$. From $KK^{tr} = K^{tr}K = mI_L$ we have $\sum_{i=1}^L k_{ij}^2 = m$ and, since $k_{ij}^2 \equiv k_{ij} \pmod 2$, $\sum_{i=1}^L k_{ij}$ is even (for all j). Hence PK has integer entries and is in $\mathbb{Z}^L$. ∎

The following corollary summarizes our results about $\mathbb{Z}^L$ for the values of L that we are interested in. Note that since $\mathbb{Z}^L$ has no "handedness", there is essentially no difference between "similar" and "strictly similar" for this lattice.

Corollary IV.1 *$\mathbb{Z}^L$ has a geometrically similar sublattice of index N if and only if*

- *N is an L^{th} power, if L is odd*
- *N is of the form $a^2 + b^2$, if $L = 2$*

- *N is of the form $m^{L/2}$ for some integer m, if $L = 4k$, $k \geq 1$*

In each case the sublattice is clean if and only if N is odd. The same results hold if "similar" is replaced by "strictly similar".

For D_4 we have only a partial answer.

Theorem IV.2 *If M is 7 or a product of primes congruent to 1 (mod 4) then D_4 has a geometrically strictly similar, clean sublattice of index M^2. The values of M mentioned are*

$$1, 5, 7, 13, 17, 25, 29, 37, 41, 53, \ldots \tag{26}$$

(7 together with Sequence A4613).

Proof. We take our standard version of the D_4 lattice to have minimal norm 2 (as in [5]) and generator matrix

$$G = \begin{bmatrix} 1 & 1 & 0 & 0 \\ -1 & 0 & 1 & 0 \\ 0 & -1 & 0 & 1 \\ 0 & -1 & 0 & -1 \end{bmatrix} . \tag{27}$$

The four rows v_1, v_2, v_3, v_4 of G correspond to the nodes of the Coxeter diagram for D_4 shown in Fig. 5, where $v_i \cdot v_i = 2$ $(i = 1, \ldots, 4)$, two nodes that are joined by an edge correspond to vectors with inner product -1, and two nodes that are not joined by an edge are orthogonal.

We regard D_4 as a subset of $\mathcal{H} = \{w + xi + yj + zk : w, x, y, z \in \mathbb{R}\}$, the space of real quaternions. Our sublattices Λ' will be constructed by multiplying D_4 either on the left or on the right by appropriate Hurwitzian integral quaternions. If $\xi = a + bi + cj + dk \in \mathcal{H}$ then ξD_4 has generator matrix GL_ξ, where

$$L_\xi = \begin{bmatrix} a & b & c & d \\ -b & a & d & -c \\ -c & -d & a & b \\ -d & c & -b & a \end{bmatrix} , \tag{28}$$

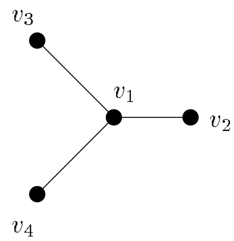

Figure 5: Coxeter diagram for any lattice that is geometrically similar to D_4: there are four generating vectors v_1, v_2, v_3, v_4 satisfying $v_1 \cdot v_1 = v_2 \cdot v_2 = v_3 \cdot v_3 = v_4 \cdot v_4$, $v_i \cdot v_j = -\frac{1}{2} v_1 \cdot v_1$ if nodes v_i and v_j are joined by an edge, and $v_i \cdot v_j = 0$ $(i \neq j)$ otherwise.

and $D_4\xi$ has generator matrix GR_ξ, where

$$R_\xi = \begin{bmatrix} a & b & c & d \\ -b & a & -d & c \\ -c & d & a & -b \\ -d & -c & b & a \end{bmatrix} . \tag{29}$$

Note that

$$L_\xi L_\xi^{tr} = R_\xi R_\xi^{tr} = m I_4, \quad L_\xi R_\xi = R_\xi L_\xi \ , \tag{30}$$

where $m = \xi \bar{\xi} = a^2 + b^2 + c^2 + d^2$.

We will show that under certain conditions ξD_4 and $D_4 \xi$ are clean sublattices. We only give the proof for $D_4\xi$, the other case being completely analogous.

The Voronoi cell for D_4 is a 24-cell, with 24 octahedral faces [4], [5]. A typical face (they are all equivalent) is that lying in the hyperplane

$$X \cdot v_1 = \frac{1}{2} v_1 \cdot v_1 \ , \tag{31}$$

having center $\delta_0 = \frac{1}{2}v_1$ and six vertices

$$\begin{aligned}
\delta_1 &= \frac{1}{2}(2v_1 + v_3 + v_4)\,, \\
\delta_2 &= \frac{1}{2}(-v_3 - v_4)\,, \\
\delta_3 &= \frac{1}{2}(2v_1 + v_2 + v_3)\,, \\
\delta_4 &= \frac{1}{2}(-v_2 - v_3)\,, \\
\delta_5 &= \frac{1}{2}(2v_1 + v_2 + v_4)\,, \\
\delta_6 &= \frac{1}{2}(-v_2 - v_4) \qquad (32)
\end{aligned}$$

(see Fig. 6). A point X belongs to this face if and only if it satisfies (31) and

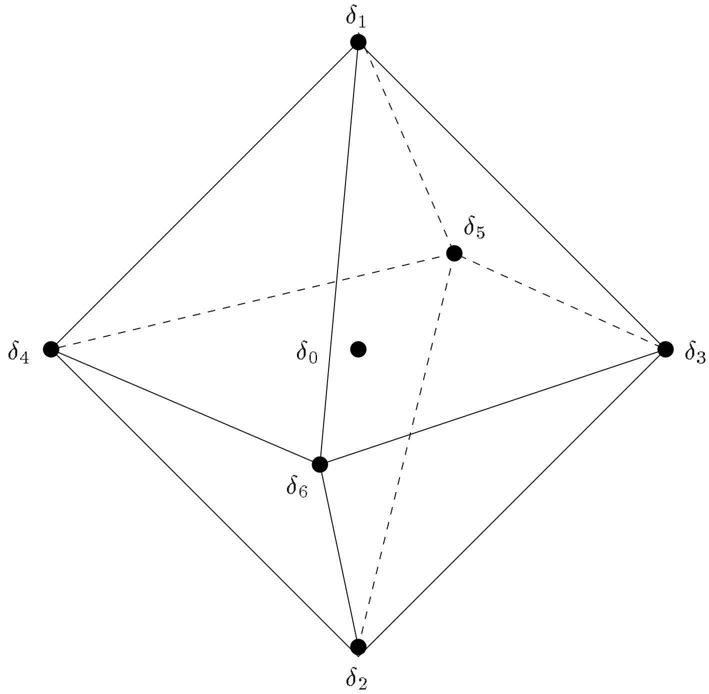

Figure 6: Labeling for center and vertices of octahedral face of Voronoi cell for D_4.

$$|(X - \delta_0)\cdot(\delta_1 - \delta_0)| + |(X - \delta_0)\cdot(\delta_3 - \delta_0)| + |(X - \delta_0)\cdot(\delta_5 - \delta_0)| \le \frac{1}{4}v_1 \cdot v_1\,. \qquad (33)$$

Let $\Lambda' = D_4\xi$, where ξ is a quaternion of the form

$$\xi = \frac{\alpha}{2} + \frac{\alpha}{2}i + \frac{\beta}{2}j + \frac{\beta}{2}k\ , \qquad (34)$$

and α and β are odd, positive, relatively prime integers. The norm of ξ is $\frac{1}{2}(\alpha^2+\beta^2)$. Then we claim that Λ' is clean.

To show this, we begin by computing the generator matrix for Λ':

$$\begin{aligned} G' &= GR_\xi \\ &= \begin{bmatrix} 0 & \alpha & 0 & \beta \\ \frac{-\alpha-\beta}{2} & \frac{-\alpha+\beta}{2} & \frac{\alpha-\beta}{2} & \frac{-\alpha-\beta}{2} \\ \frac{\alpha-\beta}{2} & \frac{-\alpha-\beta}{2} & \frac{\alpha+\beta}{2} & \frac{\alpha-\beta}{2} \\ \frac{\alpha+\beta}{2} & \frac{-\alpha+\beta}{2} & \frac{-\alpha+\beta}{2} & \frac{-\alpha-\beta}{2} \end{bmatrix}, \end{aligned} \tag{35}$$

and denote its rows by v_1', v_2', v_3', v_4'. We will similarly use primes to denote the center (δ_0') and vertices ($\delta_1', \ldots, \delta_6'$) of an octahedral face of the Voronoi cell of Λ'. From (32) we find that

$$\begin{aligned} \delta_0' &= \frac{1}{2}(0,\alpha,0,\beta), \\ \delta_1' &= \frac{1}{2}(\alpha,\alpha,\beta,\beta), \\ \delta_3' &= \frac{1}{2}(-\beta,\alpha,\alpha,\beta), \\ \delta_5' &= \frac{1}{2}(0,\alpha+\beta,0,-\alpha+\beta). \end{aligned}$$

We must show that it is impossible for a point $X=(w,x,y,z)\in D_4$ to satisfy the primed versions of (31) and (33), which are

$$\alpha x+\beta z=\frac{1}{2}(\alpha^2+\beta^2), \tag{36}$$

$$|\alpha w+\beta y|+|-\beta w+\alpha y|+|\beta x-\alpha z|\le\frac{1}{2}(\alpha^2+\beta^2). \tag{37}$$

Suppose on the contrary that $(w,x,y,z)\in D_4$ satisfies (36) and (37). From (36) we have

$$z=\frac{1}{2\beta}(\alpha^2+\beta^2-2\alpha x) \tag{38}$$

and from (37)

$$|\beta x-\alpha z|\le\frac{1}{2}(\alpha^2+\beta^2),$$

which together imply

$$\frac{1}{2}(\alpha-\beta) \le x \le \frac{1}{2}(\alpha+\beta).$$

So we may write $x = \frac{1}{2}(\alpha+\mu)$, say, where μ is an odd integer satisfying $-\beta \le \mu \le \beta$, and from (38)

$$z = \frac{\beta^2 - \alpha\mu}{2\beta} ,$$

which implies $\alpha\mu \equiv \beta^2 \pmod{2\beta}$. Since β is odd, $\beta^2 \equiv \beta \pmod{2\beta}$, and we conclude that

$$\alpha\mu \equiv \beta \pmod{2\beta} . \tag{39}$$

Thus for some integer k, $\alpha\mu - \beta = 2k\beta$, and since α and β are relatively prime, β must divide μ. Therefore $\mu = \pm\beta$. But this is impossible. For if $\mu = \beta$, $x = \frac{1}{2}(\alpha+\beta)$, $z = \frac{1}{2}(-\alpha+\beta)$, $\beta x - \alpha z = \frac{1}{2}(\alpha^2+\beta^2)$, and then (37) implies $w = y = 0$, so $w + x + y + z = \beta \notin D_4$, since β is odd. A similar argument applies if $\mu = -\beta$.

So far we have shown that if α and β are odd, positive and relatively prime, then the sublattice $D_4\xi$ is clean, where ξ is given by (34). Suppose M is a product of primes congruent to 1 (mod 4). From the classical theory of quadratic forms (see for example [6]), we know that $M = p^2 + q^2$ with p even, q odd and $gcd(p,q) = 1$. We now simply set $\alpha = p + q$ and $\beta = |p - q|$.

It remains to discuss the case $M = 7$. For this we can multiply on the left or on the right by either of the quaternions

$$\xi = \frac{1}{2} + \frac{1}{2}i + \frac{1}{2}j + \frac{5}{2}k \quad \text{or} \quad \frac{1}{2} + \frac{3}{2}i + \frac{3}{2}j + \frac{3}{2}k .$$

We omit the straightforward verification that these sublattices are clean. ■

In the other direction we have:

Theorem IV.3 *D_4 has no clean, geometrically similar sublattice of index M^2 if M is* 3, 9 *or* 11*.*

Proof. The proof is by exhaustive search, using a computer. We produced a list of all vectors of norm $2M$ in D_4, and from this we found all similar sublattices of index M^2 by finding all sets of four vectors corresponding to the Coxeter diagram of Fig. 5. Given a sublattice Λ', we compute the equations defining an octahedral face of the Voronoi cell from (31) and (33). Then AMPL [12] and CPLEX [7] were used to verify that in every case there was a point of D_4 on the face. ■

The preceding discussion has shown that the lattices $\mathbb{Z}$, $\mathbb{Z}^2$, $\mathbb{Z}^{4k}$ for $k \geq 1$ and D_4 have a plentiful supply of clean, geometrically similar sublattices. We expect the same will be true of the E_8 lattice, but this question is presently under investigation.

Finally, we remark that if Λ' is a clean sublattice of Λ and Λ'' is a clean sublattice of Λ', then Λ'' is a clean sublattice of Λ.

C Common sublattices of Λ_1 and Λ_2

We begin with a general comment. Let Λ_1 and Λ_2 be any two sublattices of a lattice Λ (they must have the same dimension as Λ but are otherwise arbitrary). Then we may form their intersection $\Lambda_\cap = \Lambda_1 \cap \Lambda_2$ and their join $\Lambda_\cup = \Lambda_1 \cup \Lambda_2$, as shown in Fig. 7. The join is the lattice generated by the vectors of both Λ_1 and Λ_2 (and in general is not simply their union). From the Second Isomorphism Theorem of group theory (e.g. [23]) the indices and

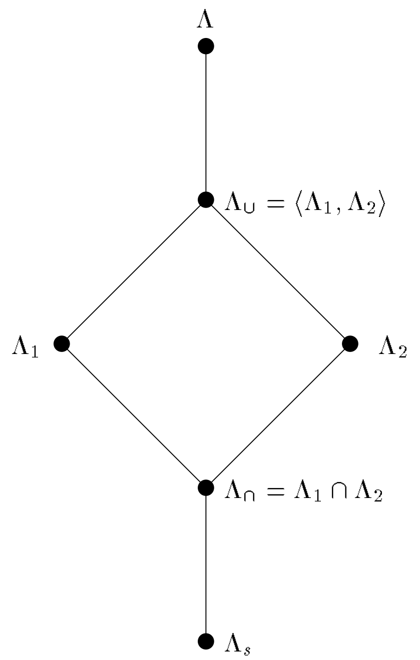

Figure 7: Intersection, join and "product" sublattice of two arbitrary sublattices.

determinants of these lattices are related by

$$[\Lambda_\cup : \Lambda_1] = [\Lambda_2 : \Lambda_\cap], \ [\Lambda_\cup : \Lambda_2] = [\Lambda_1 : \Lambda_\cap] \, , \tag{40}$$

$$\det \Lambda_1 \quad \det \Lambda_2 = \det \Lambda_\cup \quad \det \Lambda_\cap \, . \tag{41}$$

There are now in general many ways to find a "product" sublattice $\Lambda_s \subset \Lambda_\cap$ with

$$[\Lambda : \Lambda_s] = [\Lambda : \Lambda_1][\Lambda : \Lambda_2] \, . \tag{42}$$

Let Λ be one of $\mathbb{Z}$, $\mathbb{Z}^2$ or A_2, and let $\Lambda_1 = \xi_1 \Lambda$, $\Lambda_2 = \xi_2 \Lambda$ be geometrically strictly similar sublattices obtained by multiplying Λ by elements of $\mathbb{Z}$, $\mathcal{G}$ or $\mathcal{J}$ respectively. Since these three rings are unique factorization rings, the notions of greatest common divisor (gcd) and least common multiple (lcm) are well-defined. We set $\xi_\cup = gcd(\xi_1, \xi_2)$, $\xi_\cap = lcm\{\xi_1, \xi_2\}$, and then it is easy to see that $\Lambda_\cup = \xi_\cup \Lambda$, $\Lambda_\cap = \xi_\cap \Lambda$. We can also form the product sublattice $\Lambda_s = \xi_1 \xi_2 \Lambda$ (see Fig. 8). The indices of these lattices are given by

$$\begin{aligned} [\Lambda : \Lambda_1] &= (\xi_1 \bar{\xi}_1)^{L/2}, \ [\Lambda : \Lambda_2] = (\xi_2 \bar{\xi}_2)^{L/2} \, , \\ [\Lambda : \Lambda_\cup] &= (\xi_\cup \bar{\xi}_\cup)^{L/2}, \ [\Lambda : \Lambda_\cap] = (\xi_\cap \bar{\xi}_\cap)^{L/2} \, , \\ [\Lambda : \Lambda_s] &= [\Lambda : \Lambda_1][\Lambda : \Lambda_2] \, . \end{aligned} \tag{43}$$

In dimension $L = 1$, (43) implies that

$$[\Lambda : \Lambda_\cap] \ = \ lcm\{ \ [\Lambda : \Lambda_1], \ [\Lambda : \Lambda_2] \ \} \ , \tag{44}$$

and we can take $\Lambda_{lcm} = \Lambda_\cap$. However, if $L = 2$, (44) does not hold in general.

In dimensions 1 or 2, if ξ_1 and ξ_2 are relatively prime (meaning $gcd(\xi_1, \xi_2) = 1$), we have $\xi_\cup = 1$, $\xi_\cap = \xi_1 \xi_2$, $\Lambda = \Lambda_\cup$, $\Lambda_s = \Lambda_\cap$.

Because the quaternions form a noncommutative ring their arithmetic theory is more complicated. For example, it is necessary to distinguish between left gcd's and right gcd's. Both are well-defined in $\mathbb{H}_1$ and also in $\mathbb{H}_0$ as long as at least one of the quaternions involved has odd norm [8], [15]. We plan to discuss this theory and its applications to the study of sublattices of $\mathbb{Z}^4$ and D_4 elsewhere. In the present paper we will restrict our attention to

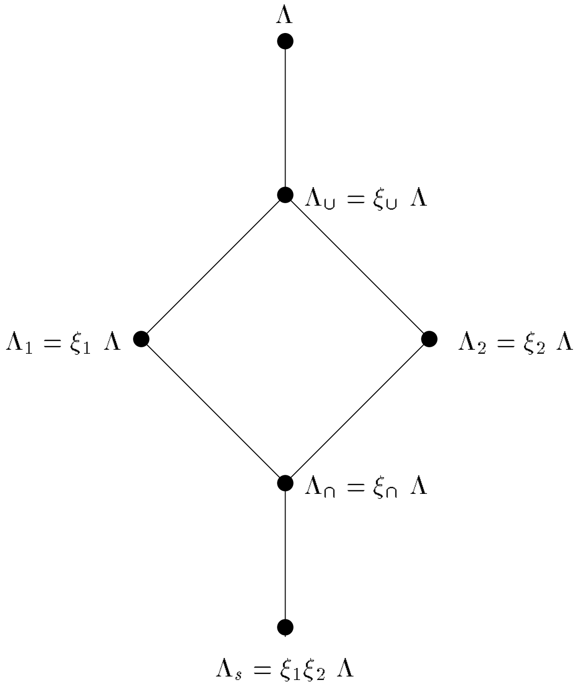

Figure 8: Join $\Lambda_\cup$, intersection $\Lambda_\cap$ and product Λ_s of two sublattices Λ_1, Λ_2 of Λ, where Λ is one of $\mathbb{Z}$, $\mathbb{Z}^2$ or A_2.

a narrow class of sublattices, which however will be general enough to provide an adequate supply of sublattices for our applications.

For $\mathbb{Z}^4$ we choose two Lipschitz integral quaternions ξ_1, $\xi_2 \in \mathbb{H}_0$ whose norms are odd and relatively prime. For D_4 we choose two Hurwitz integral quaternions

$$\begin{aligned} \xi_1 &= \frac{1}{2}\alpha_1(1+i) + \frac{1}{2}\beta_1(j+k) \in \mathbb{H}_1 \,, \\ \xi_2 &= \frac{1}{2}\alpha_2(1+i) + \frac{1}{2}\beta_2(j+k) \in \mathbb{H}_1 \,, \end{aligned} \tag{45}$$

where α_1, α_2, β_1, β_2 are odd positive integers with $gcd(\alpha_1, \beta_1) = gcd(\alpha_2, \beta_2) = gcd((\alpha_1^2 + \beta_1^2)/2, (\alpha_2^2+\beta_2^2)/2) = 1$.

In both cases we take $\Lambda_1 = \xi_1\Lambda$, $\Lambda_2 = \Lambda\xi_2$ and $\Lambda_s = \Lambda_\cap = \xi_1\Lambda\xi_2$ (see Fig. 9). Then

$$\begin{aligned} [\Lambda : \Lambda_1] &= (\xi_1\bar{\xi}_1)^2, \; [\Lambda : \Lambda_2] = (\xi_2\bar{\xi}_2)^2 \,, \\ [\Lambda : \Lambda_s] &= [\Lambda : \Lambda_1][\Lambda : \Lambda_2] \,. \end{aligned} \tag{46}$$

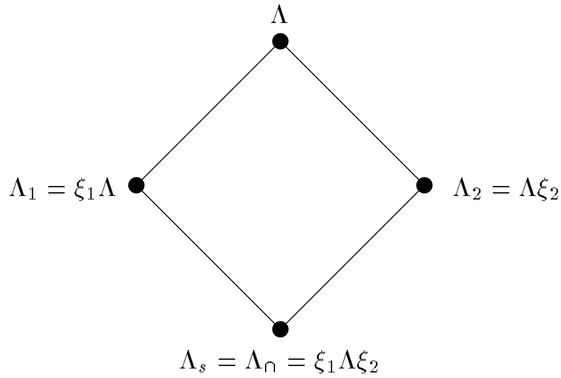

Figure 9: Λ_1 (resp. Λ_2) obtained by multiplying $\Lambda = \mathbb{Z}^4$ or D_4 on the left (resp. right) by a quaternion ξ_1 (resp. ξ_2).

For $\mathbb{Z}^4$ this gives sublattices Λ_1, Λ_2 of indices M_1^2, M_2^2, where M_1 and M_2 are any two relatively prime odd numbers (from Corollary IV.1). For D_4, M_1 and M_2 are any two relatively prime numbers from (26).

V High rate asymptotics

In this section we analyze the distortion of the asymmetric multiple description lattice quantizer at high rates.

Let $\bar{\Lambda}$ be an L-dimensional lattice with geometrically strictly similar, clean sublattices $\bar{\Lambda}_1$, $\bar{\Lambda}_2$, $\bar{\Lambda}_\cap = \bar{\Lambda}_1 \cap \bar{\Lambda}_2$, $\bar{\Lambda}_s$ (as in Figure 7), with indices $\bar{N}_1, \bar{N}_2, \bar{N}_\cap$ and $\bar{N}_s$, respectively, where $\bar{N}_s = \bar{N}_1\bar{N}_2$. It is assumed that $\nu_{\bar{\Lambda}}$, the volume of a fundamental region for $\bar{\Lambda}$, is equal to unity. A sequence of lattices is then obtained from the base set of lattices by scaling each component. Let $\Lambda_1(n) = n\bar{\Lambda}_1$, $\Lambda_2(n) = n\bar{\Lambda}_2$, $\Lambda_\cap(n) = n\bar{\Lambda}_\cap$ and $\Lambda_s(n) = n^2\bar{\Lambda}_s$. These have indices $N_1(n) = n^L\bar{N}_1, N_2(n) = n^L\bar{N}_2$ with $N_\cap(n) = n^L N_\cap$, $N_s(n) = n^{2L}N_s$ where $N_s(n) = N_1(n)N_2(n)$. As the index of the lattices grows, we scale the lattices by a factor β so that the overall rate also grows (see (59)).

We analyze the rate-distortion performance for the set of lattices $\{\Lambda, \Lambda_1(n), \Lambda_2(n), \Lambda_\cap(n), \Lambda_s(n)\}$. However, in order to keep the notation simple, we will only use the sequence index n when it is necessary to avoid confusion. Thus we will write Λ_s instead of $\Lambda_s(n)$, N_s instead of $N_s(n)$

and so on.

Referring to (11), let

$$J_s = \sum_{\lambda \in \Lambda} P(\lambda) \sum_i \gamma_i \|\lambda - \alpha_i(\lambda)\|^2. \quad (47)$$

We investigate the high-rate behavior of J_s and then find the approximation for $\bar{d}_i$, $i = 1, 2$. The latter would also allow us to predict the asymmetry in the distortion behavior of the quantizer. The reader is referred to Figure 10 for the analysis. Note that in the figure we have written $\bar{\gamma}_i = \frac{\gamma_i}{\gamma_1 + \gamma_2}$ for brevity.

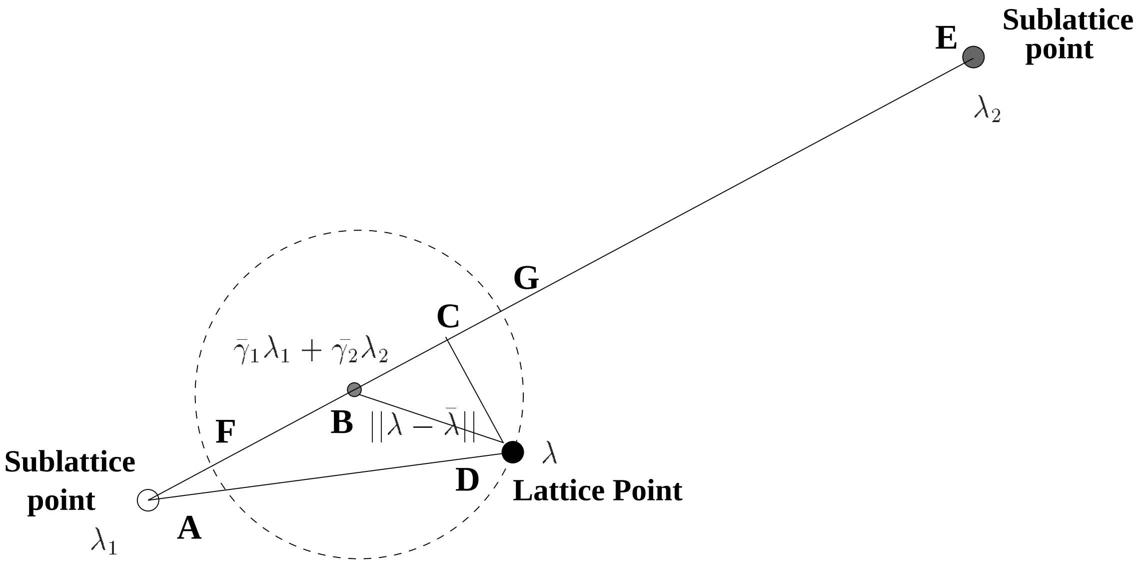

Figure 10: Relationship of edge length and distortion.

Let

$$J_{s_1} = \sum_{\lambda \in \Lambda} \frac{\gamma_1 \gamma_2}{\gamma_1 + \gamma_2} \|\alpha_2(\lambda) - \alpha_1(\lambda)\|^2 P(\lambda) \quad (48)$$

and

$$J_{s_2} = \sum_{\lambda \in \Lambda} (\gamma_1 + \gamma_2) \|\lambda - \frac{\gamma_1 \alpha_1(\lambda) + \gamma_2 \alpha_2(\lambda)}{\gamma_1 + \gamma_2}\|^2 P(\lambda). \quad (49)$$

Then, using (13),

$$J_s = J_{s_1} + J_{s_2}. \quad (50)$$

Under the assumption that $\Lambda_\cap$ is fine enough for $\text{P}(\lambda)$ to be considered a constant over $V_{\Lambda_\cap}$ we obtain

$$J_{s_1} = \frac{\gamma_1\gamma_2}{\gamma_1+\gamma_2}\sum_{\lambda'\in\Lambda_\cap}\text{P}(\lambda')\sum_{\lambda\in V_{\Lambda_\cap}(\lambda')}||\alpha_1(\lambda)-\alpha_2(\lambda)||^2. \quad (51)$$

By construction, the inner sum in (51) does not depend on λ'. Therefore, taking this out of the outer summation and using $\sum_{\lambda'\in\Lambda_\cap}\text{P}(\lambda') = 1/N_\cap$, we obtain

$$J_{s_1} = \frac{\gamma_1\gamma_2}{\gamma_1+\gamma_2}\frac{1}{N_\cap}\sum_{\lambda\in V_{\Lambda_\cap}(0)}||\alpha_1(\lambda)-\alpha_2(\lambda)||^2, \quad (52)$$

which can be written in terms of the edge endpoints as

$$J_{s_1} = \frac{\gamma_1\gamma_2}{\gamma_1+\gamma_2}\frac{1}{N_\cap}\sum_{\lambda_1\in V_{\Lambda_\cap}(0)}\sum_{\lambda_2\in V_{\Lambda_s}(\lambda_1)}\|\lambda_1-\lambda_2\|^2. \quad (53)$$

Observe that the edges in (52) are not the same as those in (53), since the points $\lambda\in V_{\Lambda_\cap}(0)$ need not be labeled using $\lambda_1\in V_{\Lambda_\cap}(0)$. However, in both cases, there is exactly one edge from each coset of $\mathcal{E}_0/\Lambda_s$. Since all edges in a coset have equal length, the sums in (52) and (53) are identical.

Using the Riemann approximation

$$\int_{V_{\Lambda_s(\lambda_1)}}||x-\lambda_1||^2 dx \approx \sum_{\lambda_2\in V_{\Lambda_s(\lambda_1)}}||\lambda_2-\lambda_1||^2\nu_2 \quad (54)$$

for the summation in (53) we obtain

$$J_{s_1} = \frac{\gamma_1\gamma_2}{\gamma_1+\gamma_2}\frac{1}{N_\cap}\sum_{\lambda_1\in V_{\Lambda_\cap}(0)}\frac{1}{\nu_2}\left[\frac{\int_{V_s(\lambda_1)}||x-\lambda_1||^2 dx}{\nu_s^{(1+2/L)}}\right]\nu_s^{(1+2/L)} \quad (55)$$

The term within the brackets is $G(\Lambda_s)$, the normalized second moment of a Voronoi cell of Λ_s ($=\frac{1}{12}$ for the square lattice), $\nu_2 = N_2$, $\nu_s = N_1N_2$ and $N_\cap/[\Lambda_1:\Lambda_\cap] = N_1$. Therefore

$$\begin{aligned} J_{s_1} &= \frac{\gamma_1\gamma_2}{\gamma_1+\gamma_2}\frac{[\Lambda_1:\Lambda_\cap]}{N_\cap\nu_2}G(\Lambda_s)\nu_s^{1+2/L} \\ &\overset{(a)}{=} \frac{\gamma_1\gamma_2}{\gamma_1+\gamma_2}G(\Lambda_s)\nu_s^{2/L} && (56)\\ &= \frac{\gamma_1\gamma_2}{\gamma_1+\gamma_2}G(\Lambda_s)(N_1N_2)^{2/L}, && (57)\end{aligned}$$

where (a) follows because $[\Lambda_1 : \Lambda_\cap] = N_\cap / N_1$ and $\nu_s = N_1 N_2$. If all the lattices in question are scaled by β, then

$$J_{s_1} = \beta^2 \frac{\gamma_1 \gamma_2}{\gamma_1 + \gamma_2} G(\Lambda_s)(N_1 N_2)^{2/L}. \tag{58}$$

The rate of the ith description is given by

$$R_i = h(p) - \frac{1}{L}\log_2(N_i) - \frac{1}{L}\log_2(\beta^L), \quad i = 1, 2. \tag{59}$$

Therefore

$$N_i = \frac{1}{\beta^L} 2^{Lh(p)} 2^{-LR_i}, \quad i = 1, 2. \tag{60}$$

The scale factor β^2 is related to the differential entropy of the source and the rate R_0 through

$$\beta^2 = 2^{2h(p)} 2^{-2R_0}. \tag{61}$$

Using (60,61) in (58) we obtain

$$J_{s_1} \approx \frac{\gamma_1 \gamma_2}{\gamma_1 + \gamma_2} G(\Lambda_s) 2^{2h(p)} 2^{-2(R_1 + R_2 - R_0)}. \tag{62}$$

A bound for J_{s_2} may be obtained in terms of $\rho_\cap$, the covering radius of $\Lambda_\cap$, by observing that for every λ, it is possible through a suitable $\Lambda_\cap$ shift to satisfy

$$\left\| \lambda - \frac{\gamma_1 \alpha_1(\lambda) + \gamma_2 \alpha_2(\lambda)}{\gamma_1 + \gamma_2} \right\| \leq \rho_\cap. \tag{63}$$

Note that[5] $\rho_\cap = \Theta(n)$ as the volume of $\Lambda_\cap$ is growing as n^L. Thus we have the inequality

$$J_{s_2} \leq (\gamma_1 + \gamma_2)\rho_\cap^2 \beta^2. \tag{64}$$

By comparing (58) and (64) we observe that $J_{s_1} = \Theta(n^4\beta^2)$ whereas $J_{s_2} = \Theta(n^2\beta^2)$. As $\nu_s = N_1 N_2 = \Theta(n^{2L})$ and $\rho_\cap = \Theta(n)$ we find that J_{s_1} dominates J_{s_2} and we obtain the approximation

$$J \approx \frac{\gamma_1 \gamma_2}{\gamma_1 + \gamma_2} G(\Lambda_s) 2^{2h(p)} 2^{-2(R_1 + R_2 - R_0)}, \tag{65}$$

where R_0 determines the central distortion $\bar{d}_0$ and is given by $\bar{d}_0 = G(\Lambda) 2^{2(h(p) - R_0)}$ (see equation (5)).

[5] Here the notation $f(n) = \Theta(g(n))$ denotes that $f(n) = O(g(n))$ as well as $g(n) = O(f(n))$. Here $f(n) = O(g(n))$ means $\limsup_{n\to\infty} |\frac{f(n)}{g(n)}| < \infty$

A Side Distortions

The approximations to the side distortions are obtained by using Figure 10 and the following analysis. The channel 1 distortion is given by

$$\bar{d}_1 = \frac{1}{N_\cap} \sum_{\lambda \in V_{\Lambda_\cap}(0)} ||\alpha_1(\lambda) - \lambda||^2 + \bar{d}_0. \tag{66}$$

Our goal is to examine the behavior of $\frac{1}{N_\cap}\sum_{\lambda \in V_{\Lambda_\cap}(0)} ||\alpha_1(\lambda) - \lambda||^2$, at high rates. To this end we write

$$\begin{aligned} ||\lambda_1 - \lambda||^2 &= ||(\lambda_1 - \bar{\lambda}) + (\bar{\lambda} - \lambda)||^2 \\ &= ||(\lambda_1 - \bar{\lambda})||^2 + ||(\lambda - \bar{\lambda})||^2 + 2\langle(\lambda_1 - \bar{\lambda}), (\bar{\lambda} - \lambda)\rangle, \end{aligned} \tag{67}$$

where $\bar{\lambda} = (\gamma_1\lambda_1 + \gamma_2\lambda_2)/(\gamma_1 + \gamma_2))$,

$$\begin{aligned} ||(\lambda_1 - \bar{\lambda})||^2 + ||(\lambda - \bar{\lambda})||^2 &- 2|\langle(\lambda_1 - \bar{\lambda}), (\bar{\lambda} - \lambda)\rangle| \leq ||\lambda_1 - \lambda||^2 \\ &\leq ||(\lambda_1 - \bar{\lambda})||^2 + ||(\lambda - \bar{\lambda})||^2 + 2|\langle(\lambda_1 - \bar{\lambda}), (\bar{\lambda} - \lambda)\rangle| \end{aligned} \tag{68}$$

and by use of the Cauchy-Schwartz inequality [18],

$$\begin{aligned} ||(\lambda_1 - \bar{\lambda})||^2 + ||(\lambda - \bar{\lambda})||^2 &- 2||(\lambda_1 - \bar{\lambda})||\ ||(\lambda - \bar{\lambda})|| \leq ||\lambda_1 - \lambda||^2 \\ &\leq ||(\lambda_1 - \bar{\lambda})||^2 + ||(\lambda - \bar{\lambda})||^2 + 2||(\lambda_1 - \bar{\lambda})||\ ||(\lambda - \bar{\lambda})||. \end{aligned} \tag{69}$$

This can be re-written as

$$\begin{aligned} ||\lambda_1 - \bar{\lambda}||^2 \left[1 - \frac{||\lambda - \bar{\lambda}||}{||\lambda_1 - \bar{\lambda}||}\right]^2 &\leq ||\lambda - \lambda_1||^2 \\ &\leq ||\lambda_1 - \bar{\lambda}||^2 \left[1 + \frac{||\lambda - \bar{\lambda}||}{||\lambda_1 - \bar{\lambda}||}\right]^2. \end{aligned} \tag{70}$$

We now justify the geometrical relationship shown in Figure 10 (note that this only holds at high rates). The main point of the analysis is that the distance $\mathrm{AD}^2 = ||\lambda - \lambda_1||^2$ is well approximated by $\mathrm{AB}^2 = ||\bar{\lambda} - \lambda_1||^2$ at high rate. Note that this need not be true on an edge-by-edge basis, but is true in an average sense as formalized below.

Summing (69) over $\lambda \in V_{\Lambda_\cap}(0)$, and using $||\bar{\lambda} - \lambda||^2 \geq 0$ we obtain

$$\begin{aligned} \sum_{\lambda \in V_{\Lambda_\cap}(0)} \left\{||\lambda_1 - \bar{\lambda}||^2 - 2||\lambda_1 - \bar{\lambda}||||\bar{\lambda} - \lambda||\right\} &\leq \sum_{\lambda \in V_{\Lambda_\cap}(0)} ||\lambda - \lambda_1||^2 \\ \leq \sum_{\lambda \in V_{\Lambda_\cap}(0)} &\left\{||\lambda_1 - \bar{\lambda}||^2 + ||\bar{\lambda} - \lambda||^2 + 2||\lambda_1 - \bar{\lambda}||||\bar{\lambda} - \lambda||\right\}. \end{aligned} \tag{71}$$

Rewriting the above equation we get

$$\left[\sum_{\lambda\in V_{\Lambda_\cap}(0)} ||\lambda_1-\bar\lambda||^2\right]\left[1-2\frac{\sum_{\lambda\in V_{\Lambda_\cap}(0)}||\lambda_1-\bar\lambda||||\bar\lambda-\lambda||}{\sum_{\lambda\in V_{\Lambda_\cap}}||\lambda_1-\bar\lambda||^2}\right]\le\sum_{\lambda\in V_{\Lambda_\cap}(0)}||\lambda-\lambda_1||^2 \quad (72)$$

$$\le\left[\sum_{\lambda\in V_{\Lambda_\cap}(0)} ||\lambda_1-\bar\lambda||^2\right]\left[1+\frac{\sum_{\lambda\in V_{\Lambda_\cap}(0)}||\bar\lambda-\lambda||^2}{\sum_{\lambda\in V_{\Lambda_\cap}(0)}||\lambda_1-\bar\lambda||^2}+2\frac{\sum_{\lambda\in V_{\Lambda_\cap}(0)}||\lambda_1-\bar\lambda||||\bar\lambda-\lambda||}{\sum_{\lambda\in V_{\Lambda_\cap}(0)}||\lambda_1-\bar\lambda||^2}\right].$$

Using these inequalities and the fact that $||\lambda-\bar\lambda||\le\rho_\cap$, we obtain the following result.

Lemma V.1 *If* $\gamma_1\neq 0,\gamma_2\neq 0$, $\lim_{R_1\to\infty}\sum_{\lambda\in V_{\Lambda_\cap}(0)}||\lambda-\lambda_1||^2=\lim_{R_1\to\infty}\sum_{\lambda\in V_{\Lambda_\cap}(0)}||\lambda_1-\bar\lambda||^2$ *when* $R_1-R_2=C$ *for some constant* C*.*

Proof: For our sequence of lattices

$$\begin{aligned}
0 &\le \lim_{R_1\to\infty}\frac{\sum_{\lambda\in V_{\Lambda_\cap}(0)}||\lambda_1-\bar\lambda||||\bar\lambda-\lambda||}{\sum_{\lambda\in V_{\Lambda_\cap}(0)}||\lambda_1-\bar\lambda||^2} && (73)\\
&\le \lim_{R_1\to\infty}\rho_\cap\frac{\sum_{\lambda\in V_{\Lambda_\cap}(0)}||\lambda_1-\bar\lambda||}{\sum_{\lambda\in V_{\Lambda_\cap}(0)}||\lambda_1-\bar\lambda||^2}\\
&= \lim_{R_1\to\infty}\rho_\cap\frac{\sum_{\lambda\in V_{\Lambda_\cap}(0)}\frac{\gamma_2}{\gamma_1+\gamma_2}||\lambda_1-\lambda_2||}{\sum_{\lambda\in V_{\Lambda_\cap}(0)}\left(\frac{\gamma_2}{\gamma_1+\gamma_2}\right)^2||\lambda_1-\lambda_2||^2}\\
&= \lim_{R_1\to\infty}\rho_\cap\left(\frac{\gamma_1+\gamma_2}{\gamma_2}\right)\frac{\sum_{\lambda\in V_{\Lambda_\cap}(0)}||\lambda_1-\lambda_2||}{\sum_{\lambda\in V_{\Lambda_\cap}(0)}||\lambda_1-\lambda_2||^2}\\
&= \lim_{R_1\to\infty}\rho_\cap\left(\frac{\gamma_1+\gamma_2}{\gamma_2}\right)\frac{\sum_{\lambda_1\in V_{\Lambda_\cap}(0)}\sum_{\lambda_2\in V_{\Lambda_s}(\lambda_1)}||\lambda_1-\lambda_2||}{\sum_{\lambda_1\in V_{\Lambda_\cap}(0)}\sum_{\lambda_2\in V_{\Lambda_s}(\lambda_1)}||\lambda_1-\lambda_2||^2}\\
&\le \lim_{R_1\to\infty}P\left(\frac{\gamma_1+\gamma_2}{\gamma_2}\right)\frac{\rho_\cap}{\nu_s^{1/L}},
\end{aligned}$$

where $P=\frac{G_1(\bar\Lambda_s)}{G(\Lambda_s)}$ is a dimensionless constant that depends on $\bar\Lambda_s$, with $G(\bar\Lambda_s)$ the normalized second moment and $G_1(\bar\Lambda_s)=\frac{\int_{V_s(\lambda_1)}||x-\lambda_1||dx}{\nu_s^{(1+1/L)}}$ is the normalized first moment. Therefore P is scale-invariant and dimensionless. Now the scaling β affects ν_s by changing it to $\nu_s\beta^L$. Also, the scaling affects $\rho_\cap$ by scaling it to $\beta\rho_\cap$. As $\frac{\rho_\cap}{\nu_s^{1/L}}=\frac{\Theta(\beta n)}{\Theta(\beta n^2)}=\Theta(n^{-1})$, we obtain $\lim_{R_1\to\infty}\frac{\rho_\cap}{\nu_s^{1/L}}=\lim_{n\to\infty}\frac{\rho_\cap}{\nu_s^{1/L}}=0$, so the expression in (73) goes to zero asymptotically in the rate. In a similar manner we can show that

$$\begin{aligned}
0 &\le \lim_{R_1\to\infty}\frac{\sum_{\lambda\in V_{\Lambda_\cap}(0)}||\bar\lambda-\lambda||^2}{\sum_{\lambda\in V_{\Lambda_\cap}(0)}||\lambda_1-\bar\lambda||^2}\le\lim_{R_1\to\infty}\rho_\cap^2\frac{N_\cap}{\sum_{\lambda\in V_{\Lambda_\cap}(0)}||\lambda_1-\bar\lambda||^2} && (74)\\
&\le G(\Lambda_s)\frac{\gamma_2^2}{(\gamma_1+\gamma_2)^2}\lim_{R_1\to\infty}[\frac{\rho_\cap}{\nu_s^{1/L}}]^2=0
\end{aligned}$$

Using these in (72) we obtain the desired result. ■

Using Lemma V.1 we can write

$$\sum_{\lambda \in V_{\Lambda_\cap}(0)} ||\lambda - \lambda_1||^2 \approx \sum_{\lambda \in V_{\Lambda_\cap}(0)} ||\lambda_1 - \bar{\lambda}||^2 = \frac{\gamma_2^2}{(\gamma_1+\gamma_2)^2} \sum_{\lambda \in V_{\Lambda_\cap}(0)} ||\lambda_1 - \lambda_2||^2 \tag{75}$$

for a sufficiently high rates. Therefore the side distortions are directly related to J_s which was calculated earlier. Hence the side distortions are approximated by

$$\begin{aligned} \bar{d}_1 &\approx \frac{\gamma_2^2}{(\gamma_1+\gamma_2)^2} G(\Lambda_s) 2^{2h(p)} 2^{-2(R_1+R_2-R_0)} \\ \bar{d}_2 &\approx \frac{\gamma_1^2}{(\gamma_1+\gamma_2)^2} G(\Lambda_s) 2^{2h(p)} 2^{-2(R_1+R_2-R_0)}. \end{aligned} \tag{76}$$

It follows that the distortion ratio, $\frac{\bar{d}_1}{\bar{d}_2}$ is approximately $(\frac{\gamma_2}{\gamma_1})^2$, a convenient formula when designing the lattice quantizer. Although this is only a high rate approximation, the examples have shown that it is also a useful formula at lower rates.

Next we examine the case when $\gamma_1 \neq 0, \gamma_2 = 0$. In this case we can show that

$$\begin{aligned} \bar{d}_1 &\approx G(\Lambda_s) 2^{2h(p)} 2^{-2R_1} \\ \bar{d}_2 &\approx G(\Lambda_s) 2^{2h(p)} 2^{-2(R_1+R_2-R_0)}. \end{aligned} \tag{77}$$

The roles are reversed when $\gamma_1 = 0$ and $\gamma_2 \neq 0$. It is worth noting that in a successive refinement scheme [10], the expression for $\bar{d}_2$ (for $\gamma_1 \neq 0, \gamma_2 = 0$) does not decay exponentially with rate, since the diameter of the set $\{\lambda : \alpha_2(\lambda) = \lambda_2'\}$ is bounded away from zero.

Let $R_0 = \frac{R_1+R_2}{2}(1+a)$, so that $R_1 + R_2 - R_0 = \frac{R_1+R_2}{2}(1-a)$. Note that a is chosen so that $a > \frac{|R_1-R_2|}{R_1+R_2}$ and therefore $R_1 + R_2 - R_0 < \min(R_1, R_2)$. Here we can clearly see the tradeoff between the central distortion $\bar{d}_0$ and the side distortions.

B Minimizing average distortion

Suppose we know that the packet loss probability on channel 1 is p_1 and the packet loss probability on channel 2 is p_2. Then the average distortion is given by

$$\bar{D} = (1-p_1)(1-p_2)\bar{d}_0 + (1-p_1)p_2\bar{d}_1 + (1-p_2)p_1\bar{d}_2 + p_1p_2\mathbb{E}[||\mathbf{x}||^2] \tag{78}$$

Using the high rate approximations developed earlier, we can find the optimal $\frac{\gamma_1}{\gamma_2}$ needed for minimizing the distortion.

Claim V.1 *The weights which minimize (78) at high rate are given by*

$$\frac{\gamma_1}{\gamma_2} = \frac{(1-p_1)p_2}{(1-p_2)p_1}. \tag{79}$$

Proof: To optimize (78) we use the high rate expressions given in (76). Using (76) in (78) we obtain

$$\bar{D} = A + B_1\left(\frac{\gamma_1}{\gamma_1+\gamma_2}\right)^2 + B_2\left(\frac{\gamma_2}{\gamma_1+\gamma_2}\right)^2, \tag{80}$$

where A, B_1, B_2 do not depend on γ_1, γ_2 (they depend on $R_1, R_2, R_0, \beta, p_1, p_2$). Without loss of generality, we can use $\bar{\gamma}_1 = \frac{\gamma_1}{\gamma_1+\gamma_2}$ and $\bar{\gamma}_2 = \frac{\gamma_2}{\gamma_1+\gamma_2}$. Hence defining $\gamma = \bar{\gamma}_1 = 1 - \bar{\gamma}_2$ and substituting in (80) we obtain

$$\bar{D} = A + B_1\gamma^2 + B_2(1-\gamma)^2. \tag{81}$$

By differentiating (81) with respect to γ and setting it to zero we obtain the given result. Note that this problem is convex (the second derivative of (81) is positive) and hence we have obtained the minimum[6] with respect to γ. ■

VI Numerical Results

In this section we illustrate the performance of the proposed quantizer and compare it to both information theoretic bounds and also the high rate asymptotic analysis developed in Section V. In comparisons of its performance with that predicted by information theory, we assume that there is an entropy (lossless) coding of the quantizer output. For a Gaussian source, the multiple description rate-distortion problem was solved by Ozarow [22], ElGamal and Cover [9].

In the first example, we design a scalar quantizer and compare its performance to the high rate asymptotic results presented in Section V. We start with a base lattice $\Lambda = \mathbb{Z}$ and use $N_1 = 5, N_2 = 3$ with $N_1(n) = 5n, N_2(n) = 3n$ for the asymptotic growth. We use a

[6] A referee pointed out an alternative way to see this result. Note that in (78) only the first three terms depend on γ_1, γ_2 and so without that term the equation is identical in form to (11) with the substitution $\gamma_1 \leftrightarrow (1-p_1)p_2, \gamma_2 \leftrightarrow (1-p_2)p_1$. Therefore $\bar{D}$ is minimized by taking $\gamma_1 = (1-p_1)p_2, \gamma_2 = (1-p_2)p_1$.

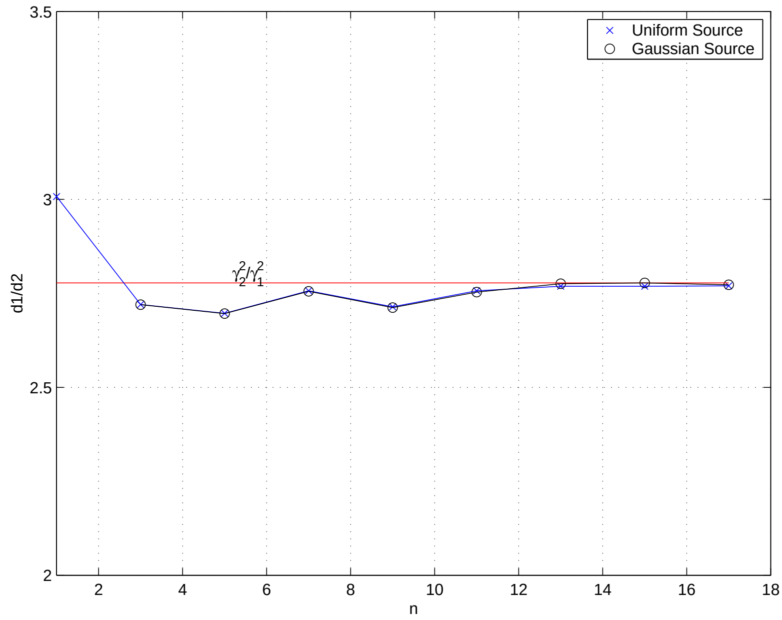

Figure 11: Comparison of side distortion ratio to $\frac{\gamma_2^2}{\gamma_1^2}$ predicted by the rate asymptotics in (76)

step size of $\beta = \frac{1}{n^3}$ to ensure that the rate scaling takes place. In Figure 11 we illustrate the rapid convergence of the distortion ratio $\frac{\bar{d}_1}{\bar{d}_2}$ to the asymptotic value $\frac{\gamma_2^2}{\gamma_1^2}$ as predicted in (76). This is shown for both Gaussian and uniform sources.

Next, in Figure 12, we compare the distortion and the rates of the quantizer to that predicted by the high rate asymptotics in (76) and (59). Each numerically obtained distortion pair is tagged with two rate pairs. The rates predicted by (59) are below the $(\bar{d}_1, \bar{d}_2)$ curve and the rates of the quantizer (numerically obtained) are above the curve. This is done for a unit variance Gaussian source. As can be seen from the figure, the high-rate predictions are quite accurate.

The vector quantizer is illustrated with the $\mathbb{Z}^2$ lattice that we described in Section III. The rates are chosen so that $R_1 - R_2 = \frac{1}{2}\log_2(\frac{|\Lambda_2|}{|\Lambda_1|})$. In Figure 13 we illustrate the tradeoff between the two side distortions by varying γ_1, γ_2. In Figure 14 we have plotted the side distortions and compared them with those predicted by information theory [22]. The key observation is that the distortion performance of the lattice quantizer is approximately 3dB away from that predicted by the rate-distortion bound. This gap is due to the shaping gain

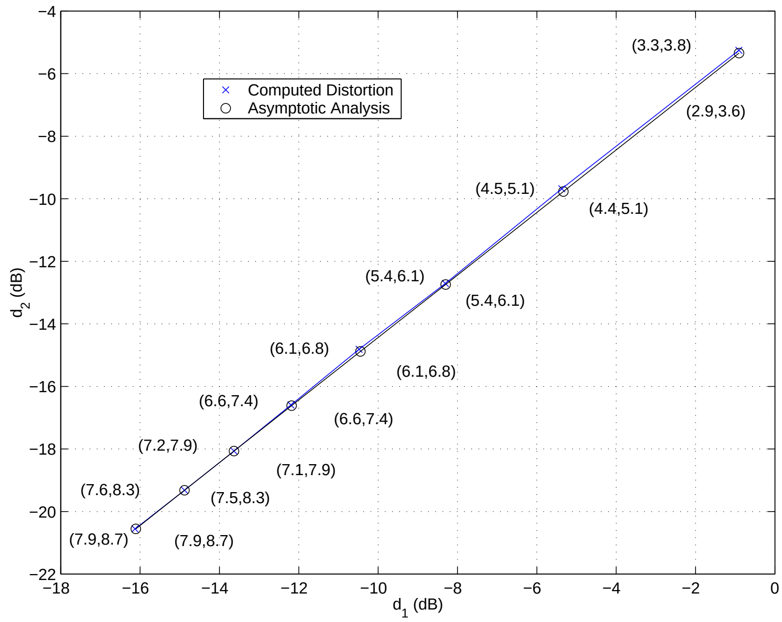

Figure 12: Comparison of side distortions and rates with the high rate asymptotics predictions in (76) and (59)

that we will pick up when we go to higher dimensions and using sublattices which have Voronoi cells which are closer to spherical. The $\mathbb{Z}^2$ lattice used in this example is more for illustrative purposes and has very little shaping gain.

VII Discussion

In this paper we have designed asymmetric multiple description lattice quantizers. This source coding scheme bridges the symmetric (balanced) multiple description quantizers and completely hierarchical successive refinement quantizers. Though a lattice vector quantizer was illustrated, this scheme could also be extended to other types of source coding schemes.

ACKNOWLEDGEMENT

We greatly appreciate the careful reading and insightful comments on the paper by the referees.

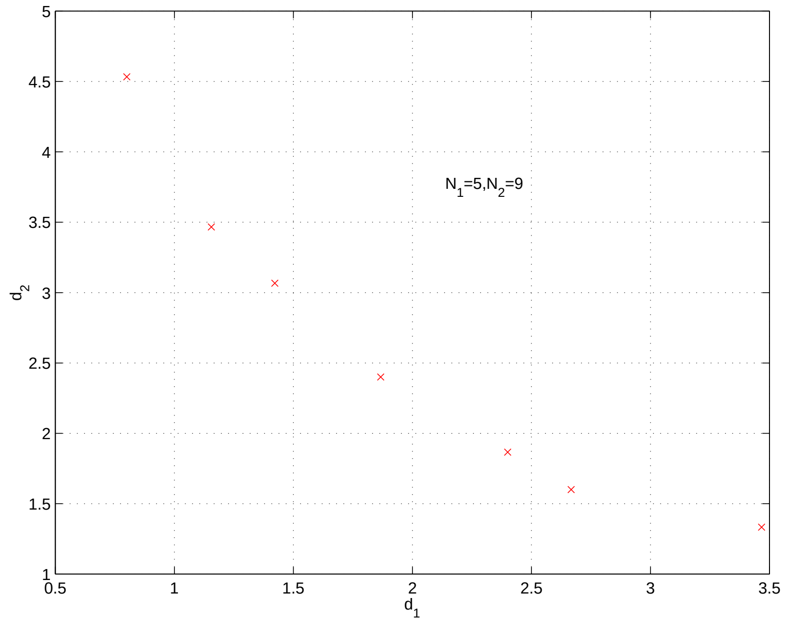

Figure 13: Side distortions for fixed sublattices with varying γ_1, γ_2.

References

[1] R. Balan, I. Daubechies and V. A. Vaishampayan, "Trading rate for distortion through varying the redundancy of a windowed fourier frame in a multiple description compression." preprint, 1999.

[2] P. A. Chou, S. Mehrotra and A. Wang, "Decoding of overcomplete expansions using projections onto convex sets," in *Proceedings, Data Compression Conference*, pp. 72–81, March 29-31 1999.

[3] J. H. Conway, E. M. Rains and N. J. A. Sloane, "On the existence of similar sublattices," *Canad. J. Math.*, vol. 51, pp. 1300–1306, 1999.

[4] J. H. Conway and N. J. A. Sloane, *The cell structures of certain lattices*, in *Miscellanea mathematica*, P. Hilton, F. Hirzebruch and R. Remmert, editors, Springer-Verlag, 1991, pp. 71–107.

[5] J. H. Conway and N. J. A. Sloane, *Sphere Packings, Lattices and Groups*, New York: Springer-Verlag, 3rd ed., 1998.

[6] D. Cox, *Primes of the Form $x^2 + ny^2$*, New York: Wiley, 1989.

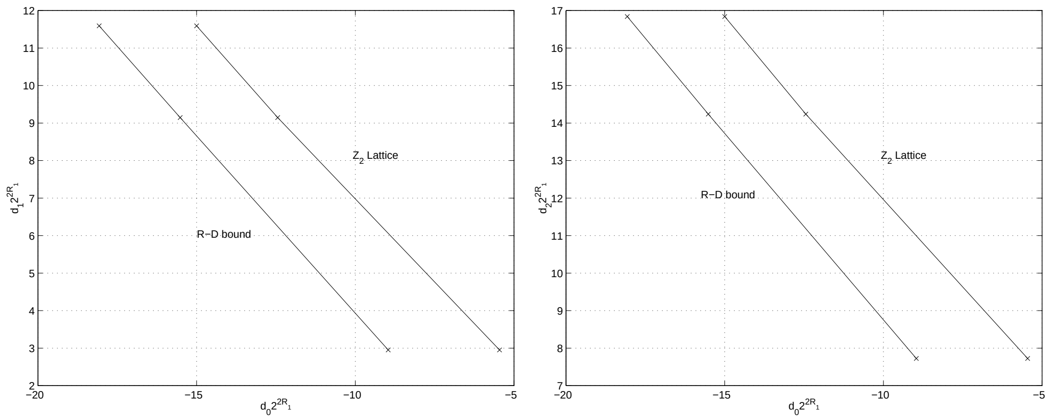

Figure 14: Comparison of lattice distortion with rate-distortion bound.

[7] *CPLEX Manual*, CPLEX Organization Inc., Incline Village, Nevada, 1991.

[8] L. E. Dickson, *Algebras and their Arithmetics*, New York: Dover, 1960.

[9] A. A. El Gamal and T. M. Cover, "Achievable rates for multiple descriptions," *IEEE Trans. Inform. Th.*, vol. IT-28, pp. 851–857, November 1982.

[10] W. H. R. Equitz and T. M. Cover, "Successive refinement of information," *IEEE Trans. Inform. Th.*, vol. 37, pp. 269–275, March 1991.

[11] M. Fleming and M. Effros, "Generalized multiple description vector quantization," in *Proceedings, Data Compression Conference*, pp. 3–12, March 29-31 1999.

[12] R. Fourer, D. M. Gay and B. W. Kernighan, *AMPL: A Modeling Language for Mathematical Programming*, Scientific Press, San Francisco, 1993.

[13] V. K. Goyal, J. Kovacevic and M. Vetterli, "Quantized frame expansions as source-channel codes for erasure channels," in *Proceedings, Data Compression Conference*, pp. 326–335, March 29-31 1999.

[14] R. M. Gray, *Source Coding Theory.* Massachusetts: Kluwer Academic Publishers, 1990.

[15] G. H. Hardy and E. M. Wright, *An Introduction to the Theory of Numbers*, Oxford: Oxford Univ. Press, 5th ed., 1980.

[16] A. Ingle and V. A. Vaishampayan, "DPCM system design for diversity systems with applications to packetized speech," *IEEE Transactions on Speech and Audio Processing*, vol. 1, pp. 48–58, January 1995.

[17] H. Jafarkhani and V. Tarokh, "Multiple description trellis coded quantizers," *IEEE Trans. Commun*, vol. 47, pp. 799–803, June 1999.

[18] D. G. Luenberger, *Linear and Non-linear programming.* Reading, Mass.: Addison-Wesley, 2nd ed., 1984.

[19] A. E. Mohr, E. A. Riskin and R. E. Ladner, "Graceful degradation over packet erasure channels through forward error correction," in *Proceedings, Data Compression Conference*, pp. 92–101, March 29-31 1999.

[20] G. Nebe and N. J. A. Sloane, *A Catalogue of Lattices*, Published electronically at *www.research.att.com/~njas/lattices/*, 2001.

[21] M. Orchard, Y. Wang, V. A. Vaishampayan and A. Reibman, "Redundancy rate distortion analysis of multiple description coding using pairwise correlating transforms," in *Proceedings of the 1997 International Conference on Image Processing*, Oct. 1997.

[22] L. Ozarow, "On a source coding problem with two channels and three receivers," *Bell Syst. Tech. J.*, vol. 59, pp. 1909–1921, December 1980.

[23] J. J. Rotman, *An Introduction to the Theory of Groups*, New York: Springer-Verlag, 4th ed., 1995.

[24] N. J. A. Sloane, *The On-Line Encyclopedia of Integer Sequences*, published electronically at *www.research.att.com/~njas/sequences.*

[25] V. A. Vaishampayan, "Vector quantizer design for diversity systems," in *Proc. Twenty-fifth Annual Conference on Information Sciences and Systems*, pp. 564–569, Johns Hopkins University, March 20–22 1991.

[26] V. A. Vaishampayan, "Design of multiple description scalar quantizers," *IEEE Trans. Inform. Theory*, vol. 39, pp. 821–834, May 1993.

[27] V. A. Vaishampayan and A. A. Siddiqui, "Speech predictor design for diversity communication systems," in *Proceedings of the 1995 IEEE Speech Coding Workshop*, 20-22 September 1995.

[28] V. A. Vaishampayan, N. J. A. Sloane and S. D. Servetto, "Multiple description vector quantization with lattice codebooks: design and analysis,", *IEEE Trans. Inform. Theory*, to appear, July 2001.

[29] J. K. Wolf, A. D. Wyner and J. Ziv, "Source coding for multiple descriptions," *Bell Syst. Tech. J.*, vol. 59, pp. 1417–1426, October 1980.

[30] Z. Zhang and T. Berger, "New results in binary multiple descriptions," *IEEE Trans. Inform. Th.*, vol. IT-33, pp. 502–521, July 1987.